Mechanisms of acid secretion and sodium uptake in H^+-ATPase-rich (HR) cell of larval zebrafish

By Khatereh Shir-Mohammadi

Supervisor: Dr. Steve Perry

Thesis submitted to the School of Graduate Studies and Research University of Ottawa in partial fulfillment of the requirements for the Master's Degree in the Ottawa – Carleton Institute of Biology

Thèse soumise à l'Ecole d'Études Superieure et de Recherché Université d'Ottawa envers la réalization partielle des éxigeances du maîtrise à l'Institut de Biologie d'Ottawa-Carleton

Abstract

Freshwater (FW) fish inhabit hypotonic environments that can vary markedly both spatially and temporally with respect to ambient salt levels and pH. Despite the chemical variability of FW, fish maintain ionic homeostasis (ionic regulation) and pH homeostasis (acid-base regulation) by manipulating ion transport mechanisms within ion-transporting cells (ionocytes) localised to the gills of adults and the skin of larvae. Ionocytes are mitochondrion-rich (MR) cells that, depending on subtype, express specific ion transporters that facilitate the movement of salts and acid-base equivalents across the gills or skin. In zebrafish (Danio rerio), one of the most well-studied ionocytes is termed the H^+-ATPase-rich (HR) cell, which is presumed to be a significant site of transepithelial Na^+ uptake/acid-secretion. Proteins that have been found in fish zebrafish HR cells include the Na^+/H^+ exchanger (NHE3), carbonic anhydrases (CA17a and CA15a), proton ATPase (H^+-ATPase) and the ammonia channel, ammonia conducting rhesus C glycoprotein b (Rhcgb), which are all thought to function in Na^+ uptake acid–base regulation. Ionic and acid-base regulation are achieved both by adjustments to the activity level of these ion transport proteins, but also by regulating the numbers of specific ionocyte subtypes (e.g. HR cells) during acclimation to environments differing in ionic composition or pH. In previous studies, the quantitative assessment of mRNA levels for genes involved in ionic and acid-base regulation relied on measurements using homogenates derived from whole body (larvae) or gill (adult). Such studies cannot distinguish whether any differences in gene expression arise from adjustments of ionocyte subtype numbers, or transcriptional regulation within individual ionocytes. Surprisingly,

there are no data on ionocyte-specific gene expression responses in zebrafish exposed to varying environments including acidic or Na^+-deficient water. To rectify this gap in the current knowledge, this thesis utilized the florescence activated cell sorting (FACS) approach to separate the HR cells from other cellular sub-populations. The technique was used to measure the gene expression of several HR cell specific transporters and enzymes in isolated HR cells from zebrafish larvae exposed to low pH (pH 4.0) or low Na^+ (5 µM) conditions. The data suggest that treatment of larvae at 4 days post fertilization with acidic water caused an increase in h^+atpase, ca17a, ca15a, nhe3b and rhcgb mRNA levels in sorted HR cells. These observations suggest the existence of multiple mechanisms of acid secretion in HR cells of larval zebrafish in acidic water; one in which acid secretion via NHE3b is linked to ammonia excretion via Rhcgb, and another facilitated by H^+-ATPase. Furthermore, these results provide molecular evidence to support roles for the CA isoforms in acid-base regulation in HR cells. On the other hand, the low Na+ treatment data suggest that nhe3b and rhcgb are the dominant genes maintaining Na^+homeostasis. In summary, the results of this thesis demonstrate that acclimation to low pH or low low Na^+ environmental conditions is facilitated by HR cell proliferation and HR cell-specific transcriptional control.

Résumé

Les poissons d'eau douce (FW) habitent dans des environnements hypotoniques qui peuvent varier nettement spatialement et temporellement en fonction des niveaux de sel et de pH, respectivement. En dépit de la variabilité d'ED, les poissons maintiennent l'homéostasie ionique (régulation ionique) et l'homéostasie de pH (régulation d'acide et de base) en manipulant les mécanismes de transport ioniques dans les cellules de transport ionique (ionocytes) localisées dans les branchies d'adultes et sur la peau de larves. Les ionocytes sont des cellules riches en mitochondries (MR) qui, dépendamment du sous-type, expriment des transporteurs ioniques spécifiques pour faciliter le mouvement de sels et d'équivalents acidiques et basiques à travers les branchies ou la peau. Dans les poissons zébrés (Danio rerio), un des ionocytes les plus étudié s'appelle cellules H^+ATPase-rich (cellules HR), qui est présumé d'être un site significatif pour l'absorption et la sécrétion transépithéliale d' Na+. Les protéines qui ont été trouvés dans les cellules HR des poissons zébrés incluent l'échangeur d'Na^+/H^+ (NHE3), des anhydrases carboniques (CA17a et CA15a), proton ATPase (H^+-ATPase) et le canal d'ammonium, et ammonia conducting rhesus C glycoprotein b (Rhcgb), qui sont tous considérés de jouer un rôle dans la régulation d'acide et de base par fonction de l'absorption d'Na^+. La régulation ionique ainsi que d'acide et de base est réalisé par l'ajustement du niveau d'activité de ces protéines de transport ionique, mais aussi par la régulation du nombre de sous-types spécifiques d'ionocytes (e.g. cellules HR) durant l'acclimation aux environnements qui diffèrent en composition d'ions ou de pH. Dans les études précédentes, l'évaluation quantitative des niveaux d'ARNm pour des gènes impliqués dans la régulation ionique ainsi que d'acide et de base se fiaient sur des mesures qui utilisaient des homogénats dérivés de corps entiers (larves) ou de branchies (adultes). Ces études

ne peuvent pas distinguer si des différences en expression génétique surviennent d'ajustements du nombre de sous-types d'ionocytes, ou de la régulation transcriptionnel dans des ionocytes individuels. Étonnamment, il n'y a pas de données sur les réactions d'expression génétique d'ionocytes spécifiques dans les poissons zébrés exposés aux environnements composé d'eau acidique ou déficiente en Na^+. Pour combler cette lacune de connaissances, cette thèse à utilisée l'approche de tri cellulaire activé par fluorescence (FACS) pour séparer les cellules HR des autres sous-populations de cellules. La technique a été utilisée pour mesurer l'expression génétique de plusieurs transporteurs et d'enzymes spécifiques aux HR s dans des cellules HR isolés provenant de poissons zébrés exposés à des conditions de bas pH (pH 4.0) ou de bas Na^+ (5µM). Les données suggèrent que le traitement des larves à 4 jours post-fertilisation avec de l'eau acidique à causé une augmentation dans les niveaux d'ARNm pour h^+atpase, ca17a, ca15a nhe3b et rhcgb dans les cellules HR triés. Ces observations suggèrent l'existence de plusieurs mécanismes de sécrétion d'acide dans les cellules HR de poissons zébrés dans l'eau acidique; une dans laquelle la sécrétion d'acide par mode de NHE3 est liée à l'excrétion par mode de Rhcgb, et une autre qui est facilité par H^+-ATPase. De plus, ces résultats fournissent la preuve moléculaire pour supporter les rôles des isoformes de CA dans la régulation d'acide et de base dans les cellules HR. D'autre part, les données du traitement de bas Na^+ suggèrent que nhe3b et rhcgb sont les gènes dominantes qui maintiennent l'homéostasie de Na^+. En résumé, les résultats de cette thèse démontrent que l'acclimation à des conditions environnementales de bas pH ou de bas Na^+ est facilité par la prolifération des cellules HR et par le contrôle transcriptionnel d' cellules HR spécifique.

Acknowledgments

I would like to begin by thanking my supervisor Dr. Steve Perry for the opportunity given to be part of his lab. He was a constant source of encouragement and valuable suggestions with various kinds of techniques in the lab.

I would also like to thank Dr. Kathleen Gilmour, Dr. Daniel Figeys and Dr. Michael Jonz for their helpful guidance. I am grateful to all members of the Perry and Gilmour labs for friendship and assistance with experiments, I am fortunate to have shared a lab space with them and I have learned so much from their experiences. I would like to especially thank Dr. Raymond Kwong, Dr.Alex Zimmer and Hong Meng Yew for their patience and willingness to answer questions.

Many thanks to Bill Fletcher, Vishal Saxena, Christine Archer, Andrew Ochalski, , Shahrukh Ghobadloo for all of their help with animal care, microscopy and flow cytometry experiments. Their hard work and willingness to help made all of my experiments possible.

I would also like to express my gratitude to my family for their love and support in all of my endeavors. Special thanks to my daughters, Mahsa and Mahya, who kept me going and my son Benyamin who is 6 months old; and to my husband, Wahid, who's continues support was always with me and finally, many thanks to my parents for supporting me at all times.

Table of content

List of Figures

List of tables:

List of abbreviation

ANOVA analysis of variance
atpv6 v-type adenosine triphosphatase 6
CA carbonic anhydrase
cDNA complementary deoxyribonucleic acid
cm centimeter
ConA concanavalin A
ct cycle threshold
DNase deoxyribonuclease
dpf days post fertilization
EDTA Ethylenediaminetetraacetic acid
FSC forward scatter
FW freshwater
g gram
h hour
H+-ATPase H+ adenosine triphosphatase
HR C H+ adenosine triphosphatase rich cell
IHC immunohistochemistry
ISH in situ hybridization
min minute
ml millilitre
mM millimolar
MitoRos MitoTrackr CMX Ros
MR/MRC mitochondrion rich cell
mRNA messenger ribonucleic acid
Na+-K+-ATPase Na+ K+ adenosine triphosphatase
NaR/NaRC Na+ K+ adenosine triphosphatase rich cell
NCC Na+ Cl- co-transporter
NHE Na+ H+ exchanger
qPCR quantitative polymerase chain reaction
real time PCR real time polymerase chain reaction
Rh Rhesus glycoprotein
SEM standard error of the mean
SSC side scatter
SIET scanning ion electrode technique
slc solute carrier family
TEP transepithelial potential xxxi
µg microgram
µl microliter
µM micromolar

Introduction

For most vertebrates, maintaining a constant body fluid osmolality is critical to survival. Teleosts living in freshwater (FW) maintain their body fluids at a much higher osmolality (i.e. ~300 mOsmol/L) than the dilute ambient medium (e.g. typically less than 1 mOsm/L) owing to the accumulation of salts. Consequently, a large outwardly directed ionic gradient leads to the continuous diffusive loss of salts to the environment largely across the gills of adults or skin of larvae. FW teleosts achieve ionic homeostasis by minimising passive salt efflux and more importantly, by the active absorption of ions from the environment. Beginning with the pioneering work of Krogh (1938), the molecular mechanisms underlying ionic regulation in FW fish have been investigated intensely for the past 80 years, the results of which are summarized in several recent reviews (e.g. Chasiotis et al., 2012; Dymowska et al., 2012; Hsu et al., 2014; Hwang, 2009; Hwang and Perry, 2010; Hwang et al., 2011; Kumai and Perry, 2012; Kwong et al., 2014).

In this thesis, I provide cell-specific molecular evidence to support the involvement of multiple enzymes and transporters thought to be crucial for ionic homeostasis in zebrafish (*Danio rerio*) larvae. The fundamental question addressed in this thesis is how the zebrafish, a FW teleost and model organism, regulates its gene activity at the cellular level when exposed to acidic or sodium deficient environments.

In this introduction, I will review three key points; 1) the power of the zebrafish model in physiological research and the current state of knowledge on mechanisms of ionic regulation and acid-base balance in this species; 2) the general consequences of low ambient pH or Na^+ on

zebrafish physiology including the associated compensatory adjustments; and 3) the pros and cons of using cell-specific methods to study transcriptional regulation in model organisms.

Zebrafish as a model system to study ionic regulation

The zebrafish, a small (about 2.5 cm in length) cyprinid species, has become a powerful model to study a variety of biological systems and phenomena. The use of zebrafish offers a number of advantages, including its relative ease to maintain in the laboratory, high fecundity, rapid development and the availability of molecular tools such as annotated genomic data and established techniques for genetic modification and generation of transgenic lines (Bill et al., 2009; Eisen and Smith, 2008; Ekker and Akimenko, 2010; Suster et al., 2009). In the laboratory, zebrafish are able to tolerate a wide range of environmental conditions, including exposure to extreme pH ranges from 4 to 10 (Horng et al., 2007), acclimation to wide range of highs and lows of ionic concentration (Nakada et al., 2007) and temperature (Chou et al., 2008), and exposure to variable levels of O_2 and CO_2 (Perry et al., 2009). Owing to their tolerance of harsh experimental treatments, combined with other advantages discussed above, the zebrafish adult and larvae has emerged as an excellent platform to investigate developmental plasticity and regulatory mechanisms of ion uptake.

Overview of zebrafish ionic regulation

Ion uptake in zebrafish larvae is dependent on salt-transporting cells termed ionocytes, which are mitochondrion-rich cells (MRC) that express specific ion transporters responsible for the movement of ions (Dymowska et al., 2012; Hwang and Chou, 2013; Hwang et al., 2011). Five types of ionocytes have been identified in zebrafish larvae thus far (for reviews see Dymowska et

al., 2012; Guh et al., 2015; Hwang and Chou, 2013), namely H^+-ATPase rich (HR) cells which are involved in H^+ extrusion and Na^+ uptake (Yan et al., 2007), Na^+/K^+-ATPase rich (NAR) cells which are enriched with Na^+-K^+-ATPase and involved in transepithelial Ca^{2+} transport (Liao et al., 2007), Na^+/Cl^- co-transporting (NCC) cells which express the Na^+-Cl^- co-transporter and are involved in both Na^+ and Cl^- uptake (Wang et al., 2009), SLC26 cells which are involved in Cl^- uptake (Bayaa et al., 2009), and K^+-secreting (KS) cells that express inwardly rectifying K^+ channels (Kir1.1) and are thought to be involved in K^+ homeostasis (Abbas et al., 2011).

While all ionocytes contribute to the overall ionic homeostasis in zebrafish, this thesis focuses specifically on HR cells. The HR cell, first identified by Lin et al. (2005), arguably is the most extensively studied and well-characterized zebrafish ionocyte, for which detailed models have been developed to explain the various cellular pathways of Na^+ uptake and acid extrusion (Fig. 1.1). Based on data from immunohistochemistry (IHC) or in situ hybridization (ISH), HR cells are known to express H^+-ATPase (*atpv6v1aa)* , sodium proton exchanger (isoform NHE3b ;*slc9a3.2)* (Yan et al., 2007), ammonia conducting rhesus C glycoprotein b (Rhcgb ,previously known as Rhcg1) (Nakada et al., 2007), carbonic anhydrase (CA) 15a (CA15a Horng and Lin, 2008) and cytosolic CA17a [previously termed CAc (Esbaugh et al., 2005) or CA2-like a (Lin et al., 2008)]. Current models propose that the HR cell is an important site of ammonia secretion via apical membrane Rhcgb (Nakada et al., 2007; Shih et al., 2008), and Na^+ uptake via NHE3b. Additionally, Na^+ uptake may occur via an unidentified Na^+ channel [potentially an acid sensing ion channel; ASIC (Zimmer et al., 2018)] coupled to H^+-ATPase (Yan et al., 2007). In either case, Na^+ uptake is intricately linked to H^+ secretion. The results of these studies, when taken together, clearly demonstrate redundancy in the functions of the HR cell with respect to Na^+ uptake and H^+

excretion, which may contribute to the ability of zebrafish to tolerate a wide range of environmental conditions to regulate ionic and osmotic homeostasis of their body fluids, which enables cellular activities and physiological processes to operate normally in this FW fish.

Effect of exposure to low sodium

Acquisition of Na^+ ions from the environment is an indispensable strategy for the survival of FW fish. As mentioned above, the HR cell is presumed to be one of two primary sites of Na^+ uptake. Several pathways have been identified for Na^+ uptake in the HR cells, the most critical of which appears to be a metabolon coupling Rhcgb and NHE3b (Kumai and Perry, 2012 Shih et al., 2012). In this particular model, Rhcgb facilitates NHE3b function by promoting NH_3 efflux and the subsequent alkalization of the external boundary layer to create a favourable H^+ gradient to achieve Na^+/H^+ exchange against an otherwise outwardly directed Na^+ gradient. In support of a compensatory role for Na^+/H^+ exchange in Na^+-deficient water, Yan et al. (2007) reported that the mRNA expression of *nhe3b* in zebrafish gills was increased in fish acclimated to low Na^+-water. The roles of the two CA paralogs in Na^+- uptake mechanisms have been investigated in zebrafish gill. The results demonstrate that when fish are acclimated to low Na^+ water, *ca15a* mRNA expression is increased, as opposed to constant levels of *ca17a* mRNA (Lin et al., 2008).

Effects of exposure to acidic water

The function of the HR cells in zebrafish is regulated in acidic (pH 4) water through an increase in cell numbers and the regulation of proteins/enzymes involved in acid-base regulation at whole animal level (Horng et al., 2007). Acclimation to an acidic environment induced a decrease of mRNA expression of *nhe3b and* an increase in *atpv6v1aa*, in the gills of adult zebrafish (Yan et al., 2007). The H^+-ATPase- and NHE3-mediated Na^+ uptake mechanisms require

a supply of intracellular H^+ that typically is provided via the hydration of CO_2, a reaction catalysed by CA17a. In addition, acclimation to acidic FW caused an increase of *ca15a* expression but did not change the *ca17a* mRNA levels in zebrafish gills (Lin et al., 2008). It was argued (Yan et al., 2007) that in acidic environments, H^+-ATPase is upregulated to enhance acid secretion to maintain internal acid–base balance, and NHE3b mRNA expression is markedly reduced because the high ambient H^+ does not favour its operation.[1]

Advantages of assessing gene expression in specific ionocyte populations

FW fish regulate ion transport to maintain body fluid ionic/osmotic homeostasis and acid-base balance as described above. Such regulation is achieved not only through the activity level of transporters, but also via the proliferation and/or differentiation of ionocytes during acclimation to environments differing in ionic composition (Hwang et al., 2011). In zebrafish, acclimation to ion (Ca^{2+}, Na^+ or Cl^-) deficient, high NH_4^+, or acidic water results in the altered expression of genes encoding ion transport proteins (Bayaa et al., 2009; Craig et al., 2007; Hoshijima and Hirose, 2007; Pan et al., 2005; Shih et al., 2008), and altered numbers of ionocyte subtypes in the skin of larvae and the gills of adults (Esaki et al., 2009; Horng et al., 2007; Shih et al., 2008). However, these types of studies cannot distinguish whether the differences in gene expression are a result of an adjustment of ionocyte subtype numbers in the skin or gill, or transcriptional regulation within individual ionocytes. To date, quantitative assessment of mRNA levels for genes involved in such environmental acclimation has relied on measurements using homogenates derived from whole body (larvae) or gill (adult). However, important biological

[1] To facilitate accurate communication in this thesis, the standard genetic nomenclature is used for all the genes used for mRNA expression analysis whenever possible

events may be masked by these traditional analytical methods owing to low signal-to-noise ratios [i.e. genes may be expressed (or regulated) in relatively few numbers of a specific ionocyte subtype compared to the vast numbers of cells from other populations], which may or may not contain the transcript of interest. Although the HR cells comprise a small percentage of cells harvested from whole larvae, they play a major role (as described above) in whole body homeostasis. Therefore, studies performed on unique populations of HR cells might allow the detection of gene transcript changes that otherwise might be obscured by high background levels in other cell types. Also, changes in one ionocyte subtype may be masked by opposite changes in another subtype. Surprisingly, there are no data on ionocyte-specific gene expression responses in zebrafish exposed to varying environments including acidic or Na^+-deficient water. To rectify this gap in the current knowledge, this thesis describes new techniques to separate the HR cells from other cellular sub-populations. The technique, once validated, was used to measure the gene expression of several HR cell specific transporters and enzymes in zebrafish larvae exposed to low pH or low Na^+ conditions.

Rationale and goals of the thesis

The current model (Fig. 1.1) of the ionic regulatory pathways in the zebrafish HR cell is outlined in detail in several recent reviews (Dymowska et al., 2012; Guh et al., 2015; Hwang and Chou, 2013; Hwang et al., 2011). The supporting data for these models were obtained predominantly using cell-specific IHC, ISH and the scanning ion electrode technique (SIET) coupled with antisense morpholino gene knockdown (Horng et al., 2007; Horng et al., 2009; Hwang et al., 2011; Shih et al., 2012; Wu et al., 2010; Yan et al., 2007). These studies were complemented by PCR analyses of mRNA levels of genes expected to be involved in ionocyte ion

uptake. However, these analyses were performed on mixed cell homogenates obtained from whole larvae or gill; data specific to different ionocyte sub-types remain lacking. Thus, there is a degree of uncertainty concerning the current HR cell model because the use of a mixed-cell population may dilute and/or mask compensatory changes in gene expression that occur only in a particular cell type. As a result, analyzing specific cell populations of high purity should provide a more accurate representation of cell-specific gene regulation. Thus, a practical strategy to enable measurements of gene expression in specific cell types is highly desirable for zebrafish research. To this end, in this thesis I use the fluorescence activated cell sorting (FACS) technique, which allows the isolation of unique cell populations. FACS serves as the cornerstone of my research, permitting the separation and identification of specific cell populations based on cell size and granularity (forward and side scatter, respectively) in concert with fluorescence labelling associated to a specific type of cell. The development of this isolation technique will allow for the first time the measurements of mRNA levels within zebrafish HR cells specifically in response to changing environmental conditions.

The overall goal of this thesis was to compare whole body and HR cell-specific changes in gene expression in zebrafish larvae exposed to different external ionic conditions. The first step was the development of a technique to dissociate and sort HR cells in larvae at 4 days post fertilization (dpf). The second step was to exploit this technique to determine the mRNA expression in HR cells after exposure to acidic or Na^+-deficient water.

Hypothesis

To demonstrate that the FACS method is capable of isolating an enriched population of HR cells using lectin Concanavalin A (ConA) as a specific marker of the apical membranes of HR cells,

I propose to examine the sorted cells using IHC with a second independent HR cell marker, an H^+-ATPase antibody. Given the current model of HR cell function (Fig. 1.1), the mRNA expression of five key target genes in the HR cell (*ca17a*, *ca15a*, *nhe3b*, the *atpv6v1aa*, and *rhcgb*) are expected to be expressed at higher levels in sorted HR cell as compared to whole fish. **I hypothesize that in low pH and low Na^+ environments, the expression of these key target genes will be regulated in HR cells to maintain the whole-body osmolality in pH and Na^+ levels, and that this regulation will occur independently of any changes in the number of HR cells**. Several specific predictions follow:

1. I predict that the low pH exposure will increase HR cell numbers because an increase in HR cell density was documented previously as a key physiological response to chronic acidic water exposure in zebrafish larvae (Horng et al., 2009). Furthermore, I predict that exposure of zebrafish larvae to acidic water will cause *atpv6v1aa* to be increased in view of its presumed dominant role in overall acid secretion (Horng et al., 2007; Horng et al., 2009) and previous reports of elevated mRNA levels in adult gill during exposure to acidic water (Chang et al., 2009; Yan et al., 2007). Predictions regarding the effects of acidic water on *nhe3b* levels are less straightforward. Two previous studies reported that acidic water exposure was associated with a reduction in *nhe3b* mRNA levels in adult gill (Yan et al., 2007; Chang et al., 2013). In zebrafish larvae, however, NHE3b activity is thought to be enhanced during exposure to acidic water as a mechanism to increase Na^+ uptake and balance the acid-induced increases in Na^+ efflux (Kumai and Perry, 2011; Kumai et al., 2011; Kwong et al., 2014). Although Kumai et al. (2011) reported stable levels of *nhe3b* levels in larvae exposed to acidic water, it was argued that the lack of any increase might have reflected the fact that whole larva mRNA was analysed. Thus, based on

theory and the weight of available evidence, it is predicted that *nhe3b* levels will increase in HR cells. It is anticipated that HR cells will express both CA paralogs to facilitate the transepithelial transport mechanisms (Hwang and Chou, 2013; Fig. 1.1). Therefore, I anticipate that both paralogs of CA will be increased because it is thought that CA17a and CA15a are involved in providing substrate (H^+) for H^+-ATPase and for fuelling NHE3b. Given that the coupling of NHE3b and Rhcgb mediates HR cell ammonia excretion via acid trapping (Hwang et al., 2011; Kumai et al., 2011; Ito et al., 2013), I predict that low pH treatment will lead to an increase in *rhcgb* because of its co-dependency with NHE3b

2. Based on previous studies, I predict that the low [Na^+] will increase HR cell numbers as a compensatory response for Na^+ deficiency (Chang et al., 2013). Previous studies has shown that the mRNA levels of *nhe3b*, *ca17 a*, and *ca15a* are increased during acclimation to low Na^+ water (Horng and Lin, 2008; Yan et al., 2007) and it is known that NHE3b, Rhcgb, and the CA isoforms form a closely associated complex of proteins that facilitates transport of ions (Esaki et al., 2009; Ito et al., 2013). Therefore, I predict that the exposure of zebrafish larvae to Na^+-deficient water, will lead to an increase of *nhe3b*, *rhcgb*, *ca17a* and *ca15a* in an attempt to facilitate Na^+ uptake to compensate for the low external Na^+ concentration. Previous studies that have evaluated the mRNA levels of *atpv6v1aa* in larvae exposed to low ambient [Na^+] have yielded conflicting results with findings of increased (Nakada et al., 2007) or decreased (Shih et al., 2012) gene expression. Considering the known stimulatory influence of H^+-ATPase activity on Na^+ uptake in zebrafish larvae (Boisen et al., 2003), I predict that HR cells will exhibit an in increase in *atpv6v1aa* levels during environmental acidification.

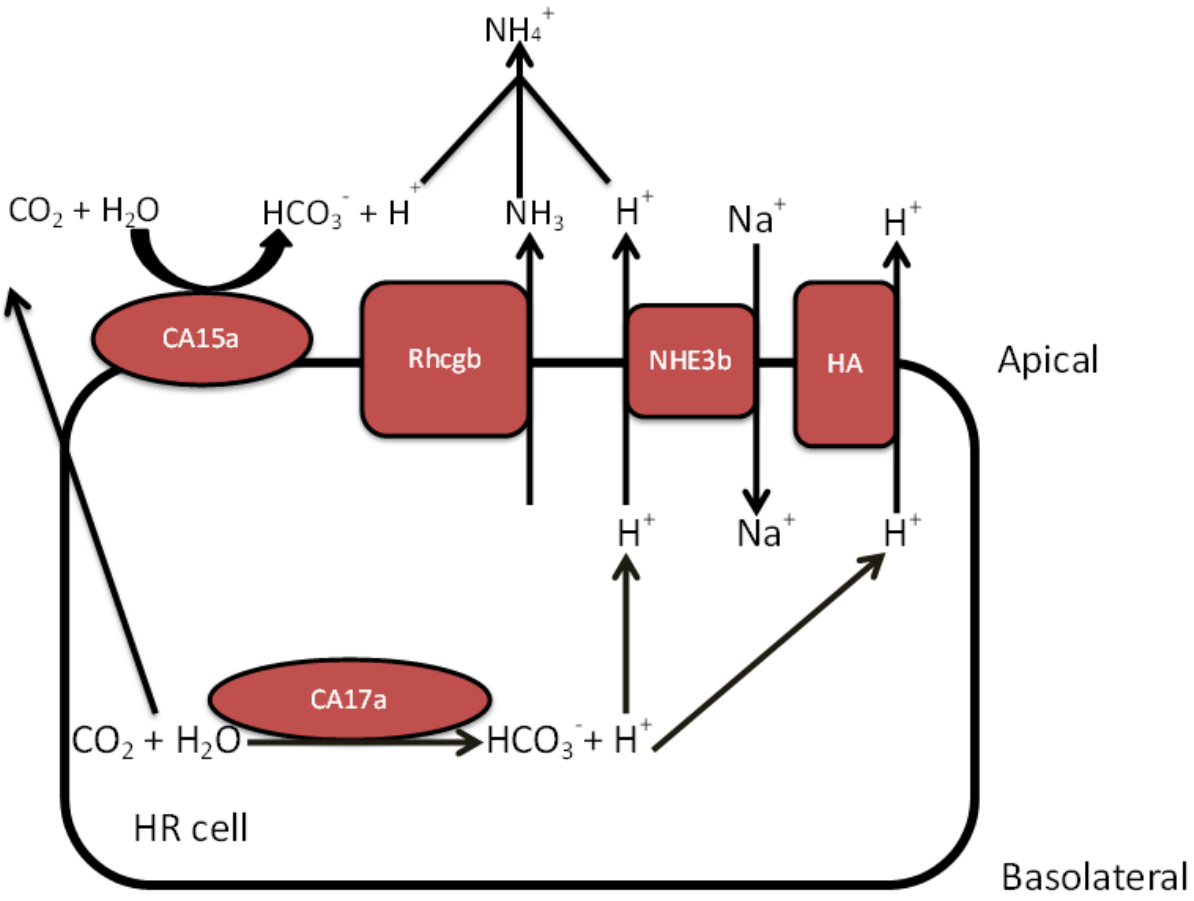
NH4+
CO2 + H2O
HCO3- + H+
NH3
H+
Na+
H+
CA15a
Rhcgb
NHE3b
HA
Apical
H+
Na+
H+
CA17a
CO2 + H2O
HCO3- + H+
HR cell
Basolateral

Figure 1.1. Diagram [modified from Hwang and Chou (2013)] illustrating the current model of Na^+ uptake and acid excretion in zebrafish HR cells. HA; V-type H^+-ATPase; NHE3b; Na^+/H^+ exchanger 3b; Rhcgb; Rhesus family C glycoprotein 1; CA17a; carbonic anhydrase 17a; CA15a; carbonic anhydrase 15a.

Material and Methods

Zebrafish

Adult zebrafish (*Danio rerio,* Hamilton-Buchanan 1822) were bred and raised in the University of Ottawa Aquatic Care Facility, where they were maintained in plastic tanks supplied with aerated, dechloraminated City of Ottawa tap water at 28° C. Fish were subjected to a constant 14 h L: 10 h D photoperiod and fed daily until satiation with No. 1 crumble-Zeigler™ (Aquatic Habitats, Apopka, FL, USA). Embryos were collected following standard protocols (Westerfield, 2000). Briefly, several male and females were placed in breeding tanks and embryos collected the next day were reared in 50 mL Petri dishes supplemented with dechloraminated City of Ottawa tap water with 0.05% methylene blue unless otherwise stated. The Petri dishes were kept in incubators set at 28.5° C. Dead embryos were removed and water was changed daily. As all experiments were performed on fish at 4 days post fertilization (dpf); they were not fed. The experiments were conducted in compliance with guidelines of the Canadian Council of Animal Care (CCAC) and after the approval of the University of Ottawa Animal Care Committee (Protocols BL-226, BL-1700).

Staining cells with Concanavalin A (ConA) and MitoTracker CMXRos (MitoRos)

The lectin Concanavalin A (ConA) was used previously as a specific marker of the apical membranes of HR cells on the skin of zebrafish larvae (Yan et al., 2007). The 4 dpf larvae were doubly stained with ConA (50 µg/L)-Alexa Fluor 488 conjugate (Invitrogen, Waltham, MA, USA) for 30 min and 1 ml of MitoRos (1 µM/µl) (579 nm excitation; Invitrogen, Waltham, MA, USA) for an additional 6 min at room temperature. The stained fish were washed and euthanized using

dechloraminated Ottawa tap water containing 4 mg/mL tricaine methanesulfonate (MS-222; Syndel Laboratories, Nanaimo, BC, Canada) in 1.05 mM Tris base, adjusted to pH 7.0 with NaOH.

Embryo/larva digestion

To form a cell suspension, 1000 whole larvae (stained with ConA and MitoRos) were transferred to a 50 mL Falcon tube (FroggaBio, North York, Ontario) and all liquid was removed completely by using 40 µm nylon mesh (Fisher Scientific co, IL, USA). Five mL of 5 mM calcium and magnesium-free ethylenediaminetetraacetic acid (EDTA) (Bioshop, Burlington, Ontario) diluted in phosphate-buffered saline (PBS) (Sigma, MO, USA) was added, and the fish were incubated for 30 min at room temperature.

The cell suspension was triturated for 2 min at room temperature to obtain a relatively homogenous solution. Cell suspensions were filtered through a 40 µm nylon mesh (Fisher Scientific co, IL, USA) into a 50 mL Falcon tube, and the digestion was subsequently stopped by adding 1 ml of Leibovitz's L-15 medium (Gibco Life Technologies, New York, USA). The isolated cells were washed 3X with L-15 medium, followed by their filtration through another 40 µm nylon mesh. The cells were pelleted by centrifugation at 1000 rpm for 5 min and the pellets were re-suspended in 5 mL of L-15 medium. The cell suspensions were then processed using fluorescence activated cell sorting (FACS).

Isolation of HR cells using fluorescence activated cell sorting (FACS)

The cell suspension was sorted using FACS (MoFlo Astrios EQ) at room temperature with lasers set at 488 and 579 nm to detect fluorescence. To minimize RNA degradation and loss of material, the sorted cells were collected directly into lysis buffer (obtained from the RNA extraction kit; see below) and when necessary, stored at −80°C. A typical FACS run of ~1000 larvae

would generate approximately 300,000 ConA positive cells, which in turn yielded approximately 250 ng of total RNA. Usually, a 3 mL sample (more than 20 million total cells) was sorted within 1 - 2 h, therefore limiting the time during which transcriptional changes in the isolated cells could occur. The optimal settings for cell sorting were determined empirically in preliminary experiments and reproduced without modification in all subsequent experiments. It is important to note that the final number of sorted HR cells was kept constant for each sort.

Flow cytometry gating strategy

Flow cytometry data analysis is built upon the principle of "gating". Gates and regions are placed around populations of cells with common characteristics, usually forward scatter, side scatter and marker expression, to investigate and to quantify these populations of interest. The first step in gating is distinguishing populations of cells based on their forward and side scatter properties. Forward and side scatter provide estimates of the size and granularity of the cells, respectively. Furthermore, it is crucial to gate for single cells and exclude doublets or clumps of cells because flow cytometry is based on single cell analysis. A step-by-step gating strategy for FACS analysis with illustrative graphs is shown in Appendix 1; each step is summarized briefly below:

1. Gating based on side and forward scatter: To distinguish populations of cells based on their forward and side scatter properties, I determined a gate by manually manipulating the gate (iterative gating) to select a region that would exclude debris and clumps of cells present in total populations of cells (Appendix 1A).

2. Gating based on the side scatter of area and height: Clumps and doublets were identified using pulse shape analysis (Wersto et al., 2001). The effectiveness of applying pulse shape analysis to gate for single cells is shown in Appendix 1B using doubly stained cells to better represent the targeted population of cells. In this plot, each data point represents an "event" which can represent single cells, doublets, clumps of cells or debris. The doublets, clumps and debris exhibit a high degree of autofluorescence and thus, ideally, they should be excluded as captured events during FACS. Re-plotting the data from Appendix 1A according to cell area and height (Appendix 1B), yields a plot in which the single cells fall along a diagonal, while the doublets, etc., exhibit increased area relative to their height. Here, I have applied the cell gate (step 1) and pulse geometry gate (step 2) to the total population of cells dissociated from 4 dpf zebrafish to yield the gated data in Appendix 1C, which should represent predominantly single events or cells.
3. Gating based on fluorescence (ConA and MitoRos): An initial experiment used a dissociated cell suspension that was divided into four aliquots, one of which was unlabelled (negative control) (Appendix 1D) to localize the negative (unstained cell) population and to define areas of background fluorescence or autofluorescence so as to set the negative gates appropriately. As shown in Appendix 1D, there were 0.2% of events exhibiting autofluorescence for the MitoRos dye; there was no detectable fluorescence for the ConA dye. Two other aliquots were stained separately with each of the dyes to determine whether there was spectral overlap between different fluorophores (ConA and MitoRos). There was 0.02 - 0.3% spectral overlap observed in singly stained cells, possibly auto fluorescence from debris (Appendix 1 E, F). One aliquot was doubly labelled for

sorting (Appendix 1G) and used in Appendix 1 A-C to clearly represent the targeted populations for each gating step.

4. Gating based on manual inspection: The shape of gate (Appendix 1G) was drawn to include events which clearly were above the background level of fluorescence, apparent from the inspection of the $ConA^+$ events (red; HR cells), $ConA^-/MitoRos^+$ events (blue; non-HR cell ionocytes) and $ConA^-/MitoRos^-$ events (purple; non-ionocytes). The thresholds set by manual inspection varied little between individual runs.

Whole larva mRNA extraction and cDNA synthesis

Total RNA was extracted from whole larvae at 4 dpf. Ten larvae were pooled to yield N = 1 and total RNA was extracted with the RNeasy Mini Kit (Qiagen, Maryland, USA) according to manufacturer's instructions. Extracted RNA was treated with DNase (Invitrogen, Waltham, MA, USA) and 1 µg of RNA subsequently reverse transcribed with the iScript cDNA Synthesis Kit (Biorad California, USA**)** according to manufacturer's instructions.

RNA extraction and cDNA synthesis for sorted cells

Total RNA was isolated from the sorted cell populations using the RNeasy Mini Kit (Qiagen, Maryland, USA), according to manufacturer's instructions. The RNA concentration and purity were determined using a Nanodrop (Biorad, California, USA). A minimum of 50 ng of total RNA was required for further processing (see below) and only samples with a 260/280 nm ratio of >1.85 were processed further. Extracted RNA was treated with DNase (Invitrogen, Waltham, MA, USA) and 50 ng of total RNA (after DNAase treatment) was used to synthesize and amplify

cDNA using the QuantiTect Whole Transcriptome Kit (Qiagen, Maryland, USA) with yields ranging from 10 to 40 µg of total cDNA.

Quantitative reverse transcription PCR (RT-qPCR)

RT-qPCR was performed using a Bio-Rad CFX96 qPCR system with SsoFast™ EvaGreen® Supermixes (Biorad, CA, USA) on all samples (cells and whole fish samples were analysed simultaneously). To allow an accurate interpretation of the data, the reaction efficiencies for each gene were determined from standard curves using pooled samples from each treatment. PCR conditions were fine-tuned until the efficiencies for each primer pair were within 90-110% to ensure that the PCR product of interest was effectively doubling with each cycle (a representative example is shown in Appendix 2). The optimum annealing temperatures of the primers were determined by temperature gradient experiments which were similar among all the primer sets; identical reactions containing a fixed primer concentration, across a range of annealing temperatures. The final PCR conditions used for all the primer pairs were as follows; 95° C for 3 min, 40 cycles of 95° C for 20 s and 58° C for 20 s, with a 5 min final extension at 72° C. All samples were assayed in triplicate. The products of the RT-qPCR were then run on a polyacrylamide gel (a representative image is shown in Appendix 3) and sequenced to confirm the specificity of the primers. Primers for the genes of interest as well as the housekeeping genes were identified from the literature (Table 2.1). For each gene, the mRNA abundance specific to HR cells ($ConA^+$), non-HR ionocytes ($MitoRos^+/ConA^-$) and non-ionocytes ($ConA^-/MitoRos^-$; hereafter referred to as negative cells) in each treatment group was calculated relative to the mRNA abundance of the negative cells from control fish. Relative mRNA expression was calculated using the delta-delta Ct method (Livak and Schmittgen, 2001), and normalized to the

mRNA abundance of the several housekeeping genes which remained constant among same treatment groups and samples used in the experiment. For the control versus low Na^+ treatment experiments, the geometric means of two housekeeping genes, *18s (NM_ 001105126.2)* and *efi1-α* (*NM_ FJ915061.1)* were used as an internal control. For control versus low pH experiments, the geometric mean of three housekeeping genes, *efi-1α*(*NM_ FJ915061.1), 18s(NM_ 001105126.2)* and α-*tubulin (tuba1c; NM_ 001105126.2)* were used for the isolated cell samples, while the geometric mean of two housekeeping genes, β-actin *(actb2: NM_181601.4)* and *efi-1α* (*NM_ FJ915061.1)* were used for the whole larvae. Relative gene expression levels were normalized to the respective levels of the controls for each treatment (pH 7.6 and 800 µM Na^+ for low pH and low Na^+ treated fish, respectively).

Immunohistochemistry on larvae and sorted cells

To verify the specificity of ConA for HR cells, larvae were exposed to ConA-Alexa Fluor 488 conjugate (50 µg/mL; Invitrogen, Waltham, MA, USA) for 30 min at room temperature and fixed using 4% paraformaldehyde (PFA) in 0.1% Tween-20 in PBS (PBS-T), followed by a stepwise dehydration to 100% MeOH In 3 X 5-min washing steps. After a stepwise rehydration in 0.1% PBS-T in three 5-min washing steps, larvae were incubated at room temperature with a solution of 3% bovine serum albumin (BSA) containing 0.8% Triton X-100 in 0.1% PBS-T for 1 h. Larvae were incubated overnight at 4° C with a rabbit primary antibody specific to a region of the A subunit of bovine HA with 100% sequence identity to the zebrafish ortholog (AEMPADSGYPAYLGAR *, NM_201135.2*), 1:4000 dilution, first used in Ura *et al*., 1996; antibody kindly provided by Professor Minoru Uchiyama) in 0.3% BSA, 0.8% Triton X-100 in 0.1% PBS-T (Kwong and Perry, 2015). Larvae were rinsed in 3 X 5-min steps in 0.1% PBS-T and incubated in donkey anti-rabbit

secondary antibody conjugated with Alexa Fluor 568 (1:500 dilution) (ThermoFisher, Burlington, ON) in 0.3% BSA, 0.8% Triton X-100 in 0.1% PBS-T. After 5 washes of 5 min each with 0.1% PBS-T, larvae were mounted on concave glass slides (Fisher Scientific, PA, USA), and images were captured using an A1R+ confocal Microscope (Nikon Instruments, Tokyo, Japan). Solid-state lasers emitting at 561 and 488 nm were used for the excitation of fluorophores; images were composed using the maximum intensity projection of Z-stacks of 30 µm total thickness composed of 10 optical sections of 3 µm each.

Dissociated cells from larvae previously stained with ConA, and sorted $ConA^{+}$ cells were fixed for 5 min using 0.4% paraformaldehyde (PFA) in 0.1% Tween-20 in PBS-T. Subsequently, both samples were incubated at room temperature in a 0.03% BSA, 0.08% Triton X-100 solution in 0.1% PBS-T for 1 h. Samples were incubated overnight at 4° C with a primary antibody specific to a region of the A subunit of bovine HA (see above; 1:4000 dilution) in 0.03% BSA, 0.08% Triton X-100 in 0.01% PBS-T. Samples were rinsed 3X and incubated in donkey anti-rabbit secondary antibody conjugated with Alexa Fluor 568 (1:5000 dilution; ThermoFisher, Burlington, ON) in 0.03% BSA, 0.08% Triton X-100 in 0.1% PBS-T for 30 min. After five washes of 5 min each with 0.1% PBS-T, both samples (total and sorted cells) were analyzed by flow cytometry (Beckman Coulter “Gallios”), with laser emissions set at 561 and 488 nm. As mentioned above, no stain (Appendix 4 A) and single stain (Appendix 4 B-C) (ConA and HA antibodies) samples also were prepared to identify the proper gate for positive and negative cells in flow cytometry.

To quantify the percentage of sorted ConA positive HR cells that also express HA, isolated cells were adhered to glass slides using poly-L-lysine (Sigma-Aldrich, MO, USA). Poly-L-lysine was thawed at room temperature and diluted into a 0.001% solution, which was then used to fully

coat Superfrost^{++} microscope slides (Fisher Scientific, PA, and USA). The microscope slides were allowed to sit at room temperature overnight. The poly-L-lysine solution was aspirated the following day and the slides were rinsed with sterile water and subsequently coated with the cells that had been fixed in PFA. The coated slides were incubated at room temperature in 0.03% BSA, 0.08% Triton X-100 solution in 0.1% PBS-T for 1 h, then left overnight at 4° C with primary HA antibody (1:4000 dilution) in 0.03% BSA, 0.08% Triton X-100 in 0.01% PBS-T. The slides were rinsed 3X and incubated in donkey anti-rabbit secondary antibody conjugated with Alexa Fluor 568 (1:5000 dilution; ThermoFisher, Burlington, ON) in 0.03% BSA, 0.08% Triton X-100 in 0.1% PBS-T for 30 min. After five washes of 5 min each with 0.1% PBS-T, the stained cells were visualised using a Nikon Eclipse Ni-U upright microscope (Nikon Instruments, Tokyo, Japan), and images were captured using an AndoriXon Ultra EMCCD camera (Andor Technology, Belfast, UK).

Experimental treatments

Fertilized embryos were transferred immediately into the appropriate treatment media after collection and maintained until 4 dpf.

Preparation of normal water *(NW)* and low sodium *(L-Na^+):* All solutions for *L-Na^+* solutions were prepared with double-deionized water supplemented with various salts (Sigma-Aldrich, St. Louis, MO). *NW* contained (in mM) 0.25 $CaCl_2$-H_2O, 0.15 $MgSO_4$, 0.005 KH_2PO_4, 0.02 K_2HPO_4 (pH 7.6) and 0.4 Na_2SO_4; *L-Na^+* water contained (in mM) 0.25 $CaCl_2$-H_2O, 0.15 $MgSO_4$, 0.005 KH_2PO_4, and 0.02 K_2HPO_4 (pH 7.6) and 0.0025 Na_2SO_4.

Preparation of low pH water: Acidic water (pH ~ 4.0) was prepared by adding H_2SO_4 (Sigma-Aldrich, MO, USA) to Ottawa tap water (pH 7.6).

Statistical analysis

All statistical analyses were performed with SigmaPlot (v. 11, Systat Inc. Chicago, IL, USA). Student's *t*-test was used to analyze flow cytometry data (i.e. cell counts between the different treatments). One-way analysis of variance (ANOVA) followed by a Holm-Sidak post hoc test was used to analyze whole fish RT-qPCR data. Two-way ANOVA followed by Holm-Sidak post hoc test was used to analyze data from RT-qPCR of sorted cells. When assumptions of normality or equal variance were not satisfied, the corresponding data were transformed using a natural log or square-root transformation. For all analyses, the level of statistical significance was determined using $p<0.05$.

Table 2.1. List of primers for RT-qPCR

Gene name	Product Length	Primer Sequence (5'-3')	Reference
actb2 (NM_181601.4)	**179**	**F: ATTGCTGACAGGATGCAGAAG** **R: GATGGTCCAGACTCATCGTACTC**	**Lin et al,.2008**
ca17a*(*NM_ BC057412)	**151**	**F: CATCTGTGCCGACCGTTGCT** **R: TTTTGTGCGTGGTTTCCCG**	**Lin et al,.2008**
ca15a (XM_017358460)	**160**	**F: TCAGAACACACTGTGGATGGC** **R: TGCTTGCTTCATTCGTTCCC**	**Lin et al,.2008**
efi1-α* (*NM_ FJ915061.1)	**101**	**F:AACAGCTGATCGTTGGAGTCAA** **R:TTGATGTATGCGCTGACTTCCT**	**Wu et al,.2012**
atpv6v1aa (NM_201135.2)	**103**	**F: GAGGAACCACTGCCATTCCA** **R:CAACCCACATAAATGATGACATCG**	**Kwong and Perry, 2016**
slc9a3.2 (XM_021468124.1)	**155**	**F: TGCAGACAGCGCCTCTAGC** **R: TGTGGCCTGTCTCTGTTTGC**	**Kwong and Perry, 2016**
rhcgb (NM_017354103.2)	**164**	**F: TCATGACACTGTTTGGGATC** **R: GCTTTTATTCAGATTGGGCC**	**Nakada et al,.2007**
***tuba1c (NM_ 001105126.2*)**	**292**	**F: CCTGCTGGGAACTGTATTGT** **R: TCA ATGAGTTCCTTG CCAAT**	**Mccurry et al,.2008**
18s (NM_ 001105126.2)	**117**	**F: GGCGGCGTTATTCCCATGACC** **R: GGTGGTGCCCTTCCGTCAATTC**	**Kumai et al,.2011**

Results

Proof of principle experiments

A first goal of this thesis was to develop, validate and optimise cell isolation and sorting techniques to obtain enriched populations of HR cells from zebrafish larvae at 4 dpf. The initial steps involved *in vivo* validation of cell-specific markers that could later be used to separate HR cells from other cell types using FACS. Thus, fish were stained with the HR-specific marker ConA (Yan et al., 2007) and MitoRos, a generic ionocyte marker (Kwong and Perry, 2016). A representative confocal microscopy image of a whole mount preparation of a 4 dpf larva doubly stained with ConA and MitoRos conjugate dyes revealed two distinct populations of cells on the cutaneous surfaces of the yolk sac and yolk sac extension (Fig. 3.1). Consistent with previous findings (Kwong and Perry, 2016) one population of cells was positive for MitoRos only, while another population exhibited co-localisation of MitoRos and ConA stain with either high or low MitoRos intensity and a population with no MitoRos or ConA stain (Negatives) (Fig. 3.1). To verify that ConA can be used as a specific marker for HR cells, specimens that were stained with ConA and MitoRos were subjected to IHC using a homologous H^+-ATPase antibody (Fig. 3.2). Approximately 97% (n = 10 individual larvae) of cells exhibited co-localization of ConA and H^+-ATPase staining (Fig. 3.2) thereby demonstrating that ConA can indeed be used as a marker for HR cells in subsequent FACS experiments.

Post-sort analyses

FACS carried out on a cell suspension that was isolated from pre-stained 4 dpf larvae revealed that signals associated with fluorescence at the expected wavelengths of 488 and 579 nm were detected in the ConA and MitoRos stained cells, respectively. FACS sorted the

suspension of total cells into three sub-populations based on fluorescence labeling of ConA and MitoRos. A representative FACS experiment (Fig. 3.3) demonstrated that 19.9% of the total yield of cells were ConA positive (HR cells) with cells exhibiting a range of MitoRos intensity, 32.9% were other ionocyte subtypes ($MitoRos^+/ConA^-$) and 37.1% were other cell types ($MitoRos^-/ConA^-$). A representative microscopy image of unsorted cells dissociated from a pool of 4 dpf larvae is shown in Fig. 3.4, clearly shows the three subpopulations [HR cells ($ConA^+$), other ionocyte subtypes ($ConA^-/MitoRos^+$) only, and non-ionocytes ($ConA^-/MitoRos^-$).

The quality of the sorted cell fractions was assessed for purity (enrichment) using flow cytometry or confocal microscopy images (positive and negative cells are counted based on the fluorescence images using at least 26 images per sort) post-FACS. A representative example of a post-sort analysis (Fig. 3.4C-E) revealed a purity of 96.3% for the sorted HR cells ($ConA^+$), 97.4% for the sorted non-HR ionocytes ($ConA^-/MitoRos^+$) and 99.4% for the non-ionocyte population ($ConA^-/MitoRos^-$). Quantification of confocal microscopy images of cells post-sorting (Fig. 3.5) demonstrated that about 95% of sorted cells were positive for ConA (n = 8 unique sorts) and thus were deemed to be HR cells. Furthermore, sorted HR cells as well as the un-sorted total population of isolated cells (control) were co-stained with ConA and HA antibody to provide an independent measure of HR cell purity after FACS. The results of both flow cytometry (Fig. 3.6) and fluorescence microscopy (Fig. 3.7) indicated that ~95% (n = 6 unique sorts) of the sorted HR cells were doubly positive for ConA and HA (i.e. they were confirmed as HR cells).

HR cell numbers for low Na^+ and low pH treatments

Flow cytometry (using ConA as the marker) was performed to determine whether the numbers of HR cells increased as a potential compensatory response when 4 dpf larvae were

exposed to Na^+-deficient water (Fig. 3.8) or low environmental pH (Fig. 3.9). Larvae reared under low Na^+ conditions exhibited a significantly higher percentage of HR cells (27.9% of total isolated cells) than in the cell populations isolated from fish reared in control water (19.2% of total isolated cells; Fig. 3.8). Similarly, the percentage of HR cells was significantly higher (Fig. 3.9) in total cell populations that were isolated from larvae reared at pH 4 (~29.9%) as compared to larvae maintained at pH 7.6 (~20.8%).

Effects of low Na^+ or low pH exposure on H^+-ATPase (*atpv6v1aa*) mRNA expression in whole larvae and isolated cells

Relative transcript abundances of *atpv6v1aa* were assessed by real-time RT-PCR using cDNA obtained from whole fish homogenates or cDNA obtained from three distinct populations of sorted cells; HR cells, other MitoRos positive ionocytes and other non-ionocyte cells in control zebrafish larvae and larvae that were exposed to low [Na^+] (5 µm Na^+) or acidic water (pH 4).

The low Na^+ treatment did not affect the expression levels of *atpv6v1aa* in whole larvae (P value of 0.21) (Fig. 3.10A). The relative transcript abundance of *atpv6v1aa* was significantly elevated in HR cells relative to the non-HR ionocyte and non-ionocyte fractions (P value <0.001). There was no significant effect of exposure to low [Na^+] in any of the three sorted cell fractions (P value of 0.237,0.200, 0.917 for HR vs. negative, HR vs. MitoRos and MitoROs vs. negative respectively) (Fig. 3.10B). On the other hand, low pH treatment elevated the mRNA abundance of *atpv6v1aa* by 5-fold in whole larvae (P value 0.010) (Fig. 3.10C), 8-fold in HR cells and 2-fold in the non-HR ionocytes with P value of 0.021 (Fig. 3.10D); the non-ionocyte population was unaffected by either treatment with p value of 0.918.

Effects of low Na^+ or low pH exposure on NHE3b (*slc9a3.2*) expression in whole larvae and isolated cells

The relative transcript abundance of *nhe3b* was significantly elevated in HR cells relative to the non-HR ionocyte and non-ionocyte fractions (P value 0.005). The levels of *nhe3b* were elevated by low Na^+ exposure when assessed in whole larvae (2-fold, P value 0.025) but the increase in mRNA was much greater in isolated HR cells (7-fold, P value<0.001) (Fig. 3.11A, B). The non-HR cells ionocytes and the non-ionocyte populations were unaffected by exposure to acidic water (Fig. 3.11B (P value of 0.08 and 0.23 respectively). Unlike for low [Na^+], the low pH treatment did not affect the expression levels of *nhe3b* in whole larvae (P value 0.818) (Fig. 3.11C). However, the transcript abundance of *nhe3b* was significantly elevated by 4-fold in HR cell ionocytes (P-value <0.001) (Fig. 3.11D); the non-HR cell ionocyte and the non-ionocyte populations were unaffected by acidic water treatment (P-value 0.101 and 0.436 respectively).

Effects of low Na^+ or low pH exposure on Rh family C glycoprotein b (*rhcgb*) expression in whole larvae and isolated cells

The relative expression of *rhcgb* was higher in ionocytes (HR and non-HR cells) relative to the non-ionocyte fraction (Fig. 3.12). The mRNA expression of *rhcgb* was elevated by low Na^+ exposure in whole larvae (10-fold, P value <0.001) and this effect was increased to a lower extent in isolated HR cells (4.2-fold, P value 0.04)) (Fig. 3.12A, B). Interestingly, the low Na^+ treatment also significantly elevated the expression of *rhcgb* in the non-ionocyte fraction by 7 folds (P value 0.02) (Fig. 3.12B).

The mRNA expression of *rhcgb* was increased after exposure to low pH in whole larvae (5-fold P-value<0.001) as well as in the isolated HR cell population (15-fold, P value 0.015) (Fig. 3.12C, D) as well as in the non-ionocyte fraction (3-fold, P value 0.032).

Effects of low Na^+ or low pH exposure on *ca17a* and *ca15a* expression in whole larvae and isolated cells

The expression of c*a15a* was significantly elevated in the sorted HR cells relative to the non-HR ionocytes and non-ionocytes (P value <0.001) (Fig. 3.13). No significant increases were observed in *ca15a* expression in whole larvae or isolated cells (including HR cells) when fish were exposed to low Na^+ (Fig. 3.13A, B) (P value 0.32). However, the expression of *ca15a* was elevated after exposure of fish to low pH in whole larvae (5-fold, P-value 0.017) yet to a much greater extent in isolated HR cells (10-fold P value 0.01); the other cell types were unaffected with P-value of 0.370 and 0.343 for MitoRos and Negative samples respectively (Fig. 3.13C, D).

Similar to c*a15a*, the expression of *ca17a* was significantly elevated in the sorted HR cells relative the non-HR ionocytes and non-ionocytes (P value <0.001)(Fig. 3.14). Consistent with the ca15a data, no significant changes in *ca17a* expression levels were induced by low Na^+ treatment in either whole larvae or isolated HR cells (P value 0.34 and 0.45 respectively) (Fig. 3.14A, B). However, the *ca17a* expression levels increased after low pH treatment in both whole larvae (5-fold) and to a greater extent in isolated HR cells (23-fold, P-value of 0.012) (Fig. 3.14C, D) with no significant changes in non-HR cells cell fraction with P-value of 0.359 and 0.721 for MitoRos and Negative samples respectively.

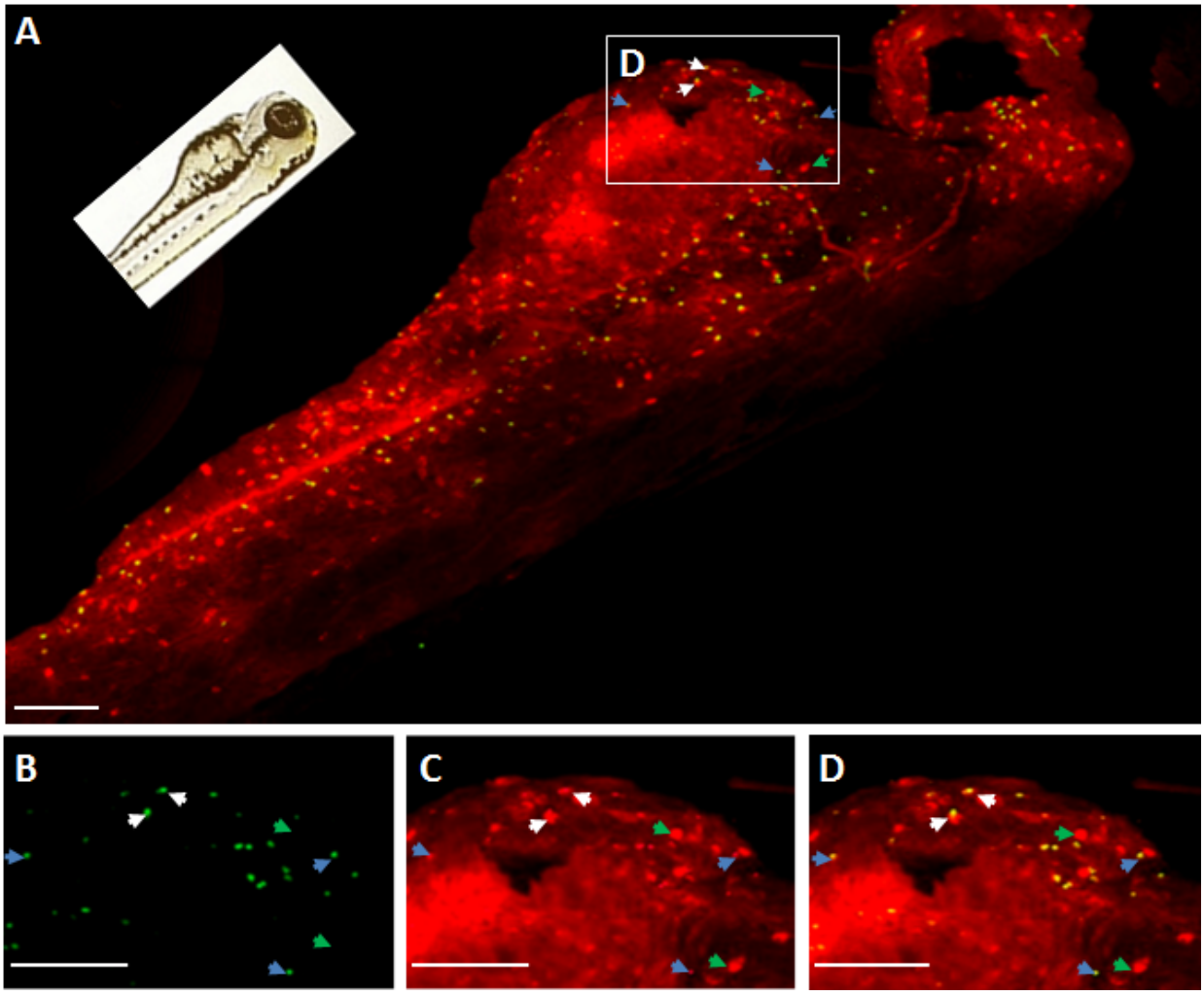
A
D
B
C
D

Figure 3.1. Representative confocal microscopy images of Concanavalin A (ConA; green) and MitoTracker CMXRos (MitoRos; red) stained cells on the skin of a wild type 4 dpf zebrafish (*Danio rerio*) larva. (A) The merged images revealed cells that either co-expressed ConA and MitoRos or cells that were positive only for MitoRos. (B) An enlarged image of a selected yolk sac region showing ConA staining. (C) An enlarged image of a selected yolk sac region showing MitoRos staining. (D) An enlarged image of a selected yolk sac region showing co-localization of ConA and MitoRos. White arrows indicate cells positive for ConA with high intensity of MitoRos stain, blue arrows indicate cells positive for ConA and low intensity of MitoRos stain and the green arrows indicate cells positive for MitoRos only. Scale bars represent 100 µm.

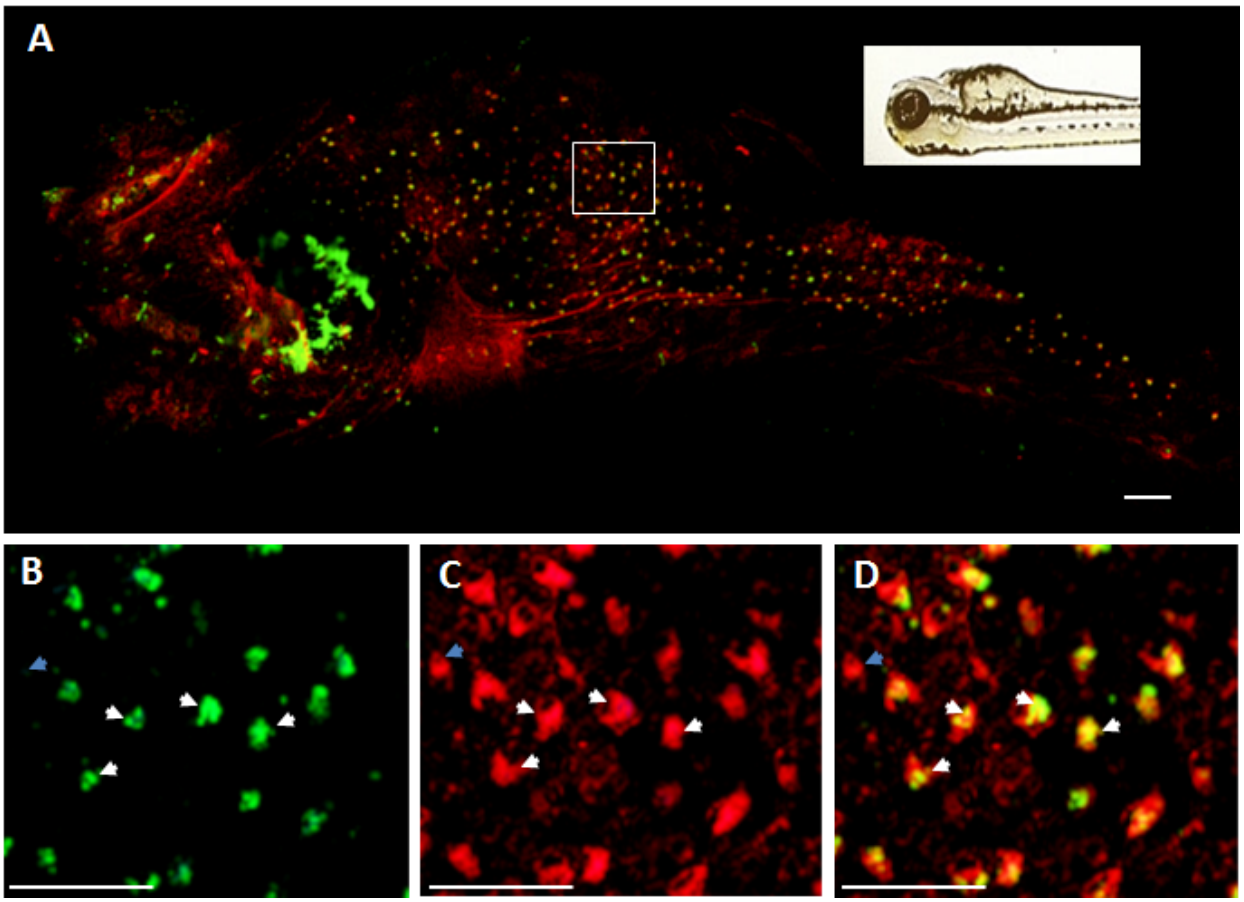
A
B
C
D

Figure 3.2. Representative confocal microscopy images of Concanavalin A (ConA; green) and H^+-ATPase (HA; red) stained cells on the skin of a wild type 4 dpf zebrafish (*Danio rerio*) larva. (A) Double immunofluorescence staining for ConA and HA indicates co-expression of ConA and HA in nearly all of the stained cells. (B) An enlarged image of a selected yolk sac region showing ConA staining. (C) An enlarged image of a selected yolk sac region showing HA staining. (D) An enlarged image of a selected yolk sac region showing co-localization of ConA and HA. The white arrows indicate cells co-expressing ConA and HA, blue arrows indicate cells positive for only HA. Scale bars represent 50 µm.

A

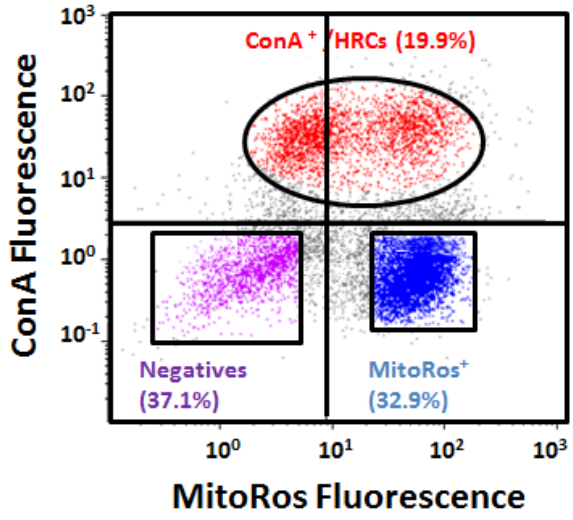

B

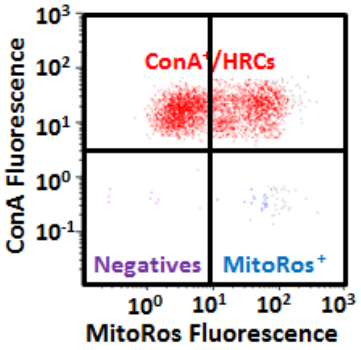

Gate	%Gate
All	100.00
ConA⁺/HRCs	96.3
MitoRos⁺	0.6
Negatives	3.1

D

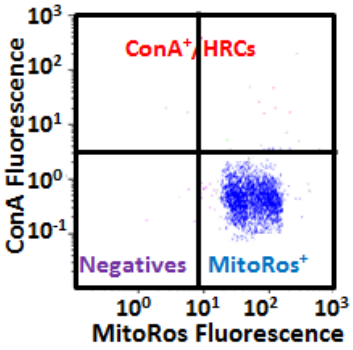

Gate	%Gate
All	100.00
ConA⁺/HRCs	0.4
MitoRos⁺	97.4
Negatives	2.2

C

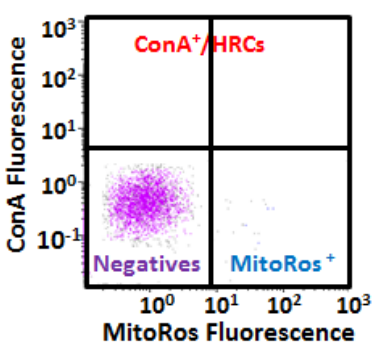

Gate	%Gate
All	100.00
ConA⁺/HRCs	0.6
MitoRos⁺	0.02
Negatives	99.4

Figure 3.3. **Representative analytical results obtained during (A) fluorescence activated cell sorting (FACS) of cells isolated from zebrafish (*Danio rerio*) larvae (*Danio rerio*) at 4 dpf and (B-D) during post-sort flow cytometry using the cells isolated by FACS.** Cells were separated into three distinct populations based on fluorescence intensity of ConA and MitoRos, using the sorting gates determined by the non-stain and single stain controls (presented in Appendix 1). (A) Three populations of cells were sorted as indicated by the different colours; $ConA^+$ cells (HR cells; red), $MitoRos^+/ConA^-$ cells (non-HR ionocytes; blue) and $MitoRos^-/ConA^-$ cells (non-ionocytes; purple). (B-D) Representative flow cytometry data using cells obtained by FACS (A). Post-sort analysis revealed a purity of ~96.3% for HR cells ($ConA^+$), 97.4% for non-HR ($MitoRos^+/ConA^-$) ionocytes, and 99.4% for non-ionocytes ($MitoRos^-/ConA^-$).

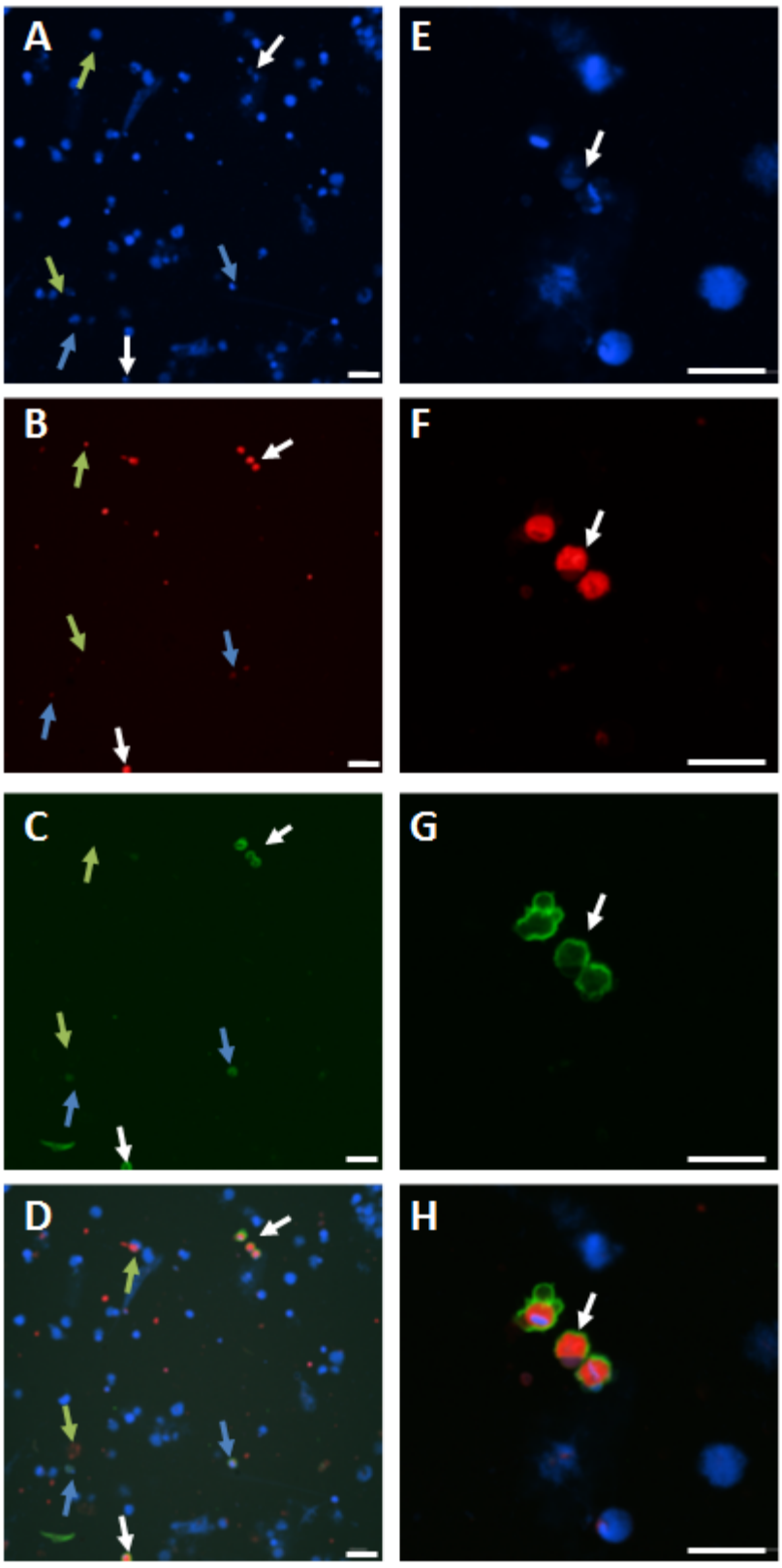
A
E
B
F
C
G
D
H

Figure 3.4. Representative fluorescence microscopy images of unsorted dissociated cells from a pool of zebrafish *(Danio rerio*) larvae at 4 dpf. (A & E) DAPI (4',6-diamidino-2-phenylindole) staining (blue) showing cell nuclei. (B & F) MitoTracker Red CMXRos (MitoRos) staining (red) of mitochondrion rich cells. (C & G) Concanavalin A (ConA) staining (green) of apical membranes of H^+-ATPase rich cells (HR cells). (D & H) Colocalization of DAPI, MitoRos and ConA, I; blue arrows indicate cells positive for DAPI, ConA and low intensity of MitoRos staining, the green arrows indicate cells positive for DAPI and high intensity MitoRos staining, and the white arrows indicate cells positive for DAPI, high intensity of MitoRos and ConA. Scale bars represent 20 µm.

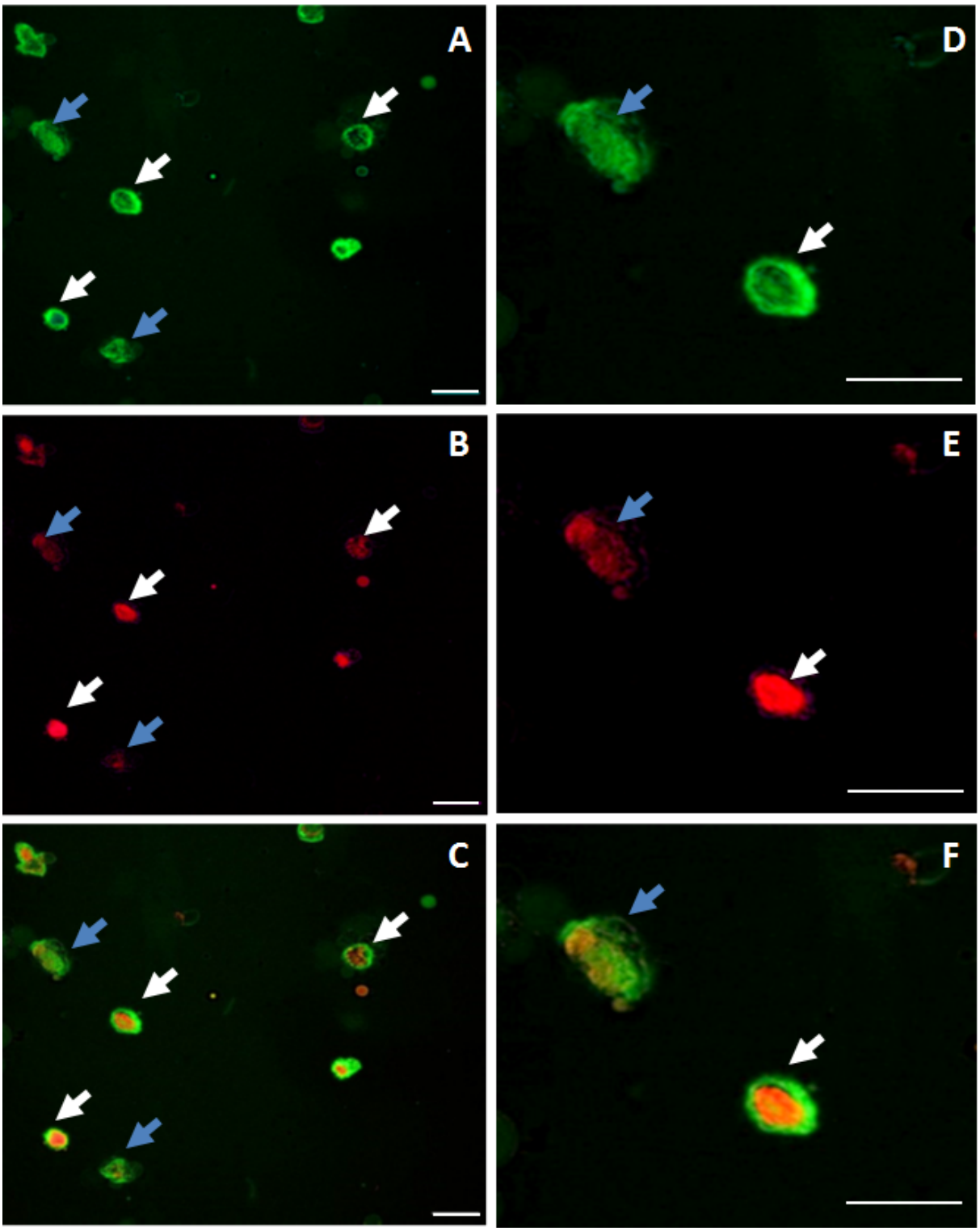
A
D
B
E
C
F

Figure 3.5. Representative fluorescence microscopy images of an enriched population of putative HR cells obtained after sorting (FACS) of dissociated cells from a pool of zebrafish *(Danio rerio*) larvae at 4 dpf. Sorted cells displayed positive staining for (A) ConA (green) and (B) MitoRos (red). Co-expression of ConA and MitoRos was demonstrated by overlaying the red and green fluorescence channels (C). Magnified images of two cells are included to demonstrate the two patterns of ConA/MitoRos co-localization in the putative HR cells isolated by FACS (D-F). White arrows indicate cells positive for ConA and exhibiting a high intensity of MitoRos staining; the blue arrows indicate cells positive ConA with a low intensity of MitoRos staining. Scale bars represent 20 μm.

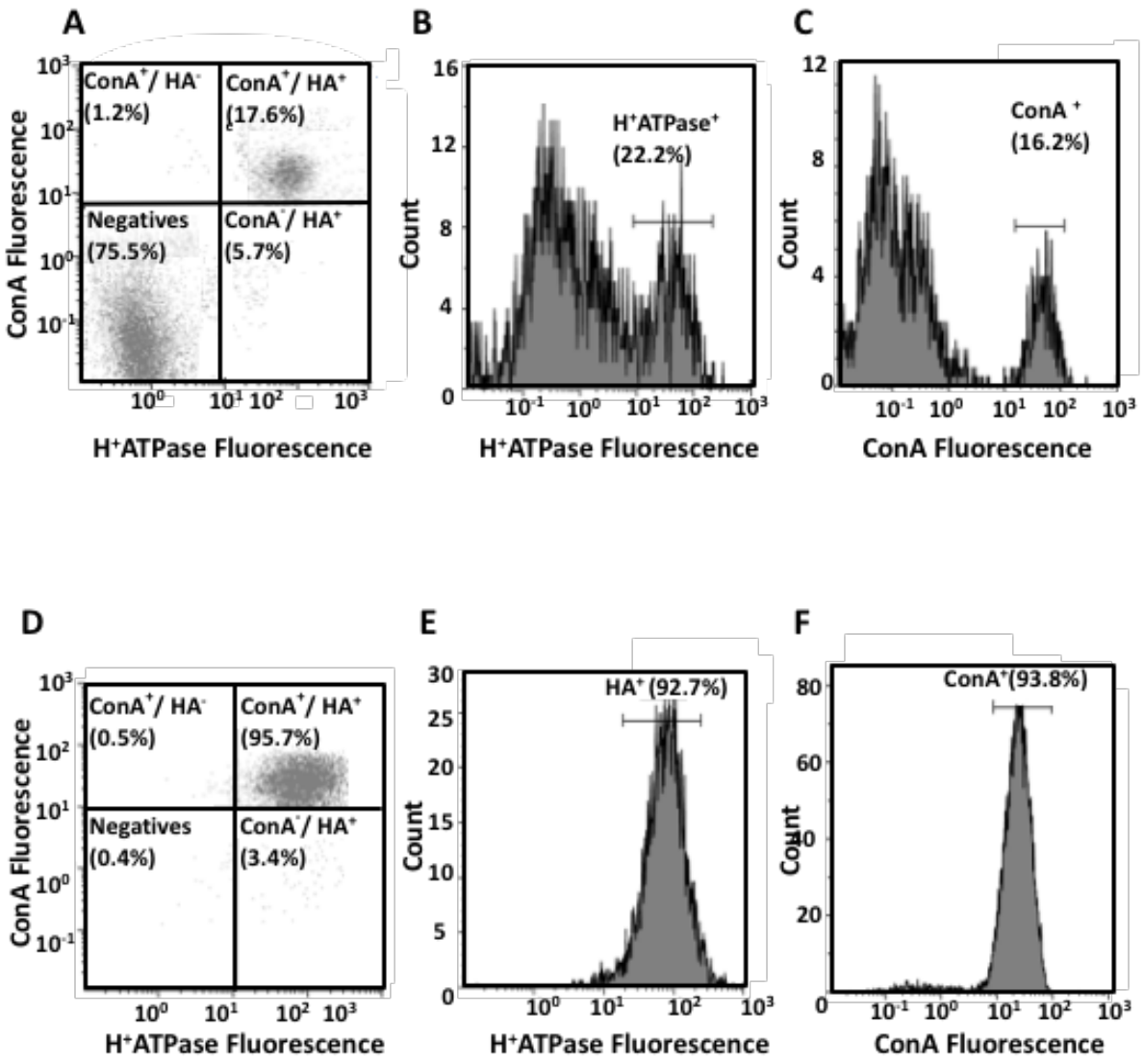
A
ConA+/ HA-
(1.2%)
ConA+/ HA+
(17.6%)
Negatives
(75.5%)
ConA-/ HA+
(5.7%)
ConA Fluorescence
H+ATPase Fluorescence
B
H+ATPase+
(22.2%)
Count
H+ATPase Fluorescence
C
ConA +
(16.2%)
Count
ConA Fluorescence
D
ConA+/ HA-
(0.5%)
ConA+/ HA+
(95.7%)
Negatives
(0.4%)
ConA-/ HA+
(3.4%)
ConA Fluorescence
H+ATPase Fluorescence
E
HA+ (92.7%)
Count
H+ATPase Fluorescence
F
ConA+(93.8%)
Count
ConA Fluorescence

Figure 3.6. Representative flow cytometry data verifying (using H^+-ATPase (HA) post-staining) the enrichment of HR cells by FACS performed on cells isolated from zebrafish (*Danio rerio*) larvae (*Danio rerio*) at 4 dpf. Cells were obtained from **(**A-C) unsorted cells and (D-F) sorted cells obtained by FACS. The unsorted cells contained 17.6% of $ConA^+/HA^+$ cells (HR cells) as determined by (A) scaterplot analysis. Histogram fluorescence analysis (B, C) revealed that the HA^+ and $ConA^+$ cells represented 22.2 and 16.2%, respectively, of the total cell population. The sorted cells contained 95.7% of $ConA^+/HA^+$ cells (HR cells) as determined by (D) scaterplot analysis. Histogram fluorescence analysis (E, F) revealed that the HA^+ and $ConA^+$ cells represented 92.7% and 93.8%, respectively, of the sorted cell population.

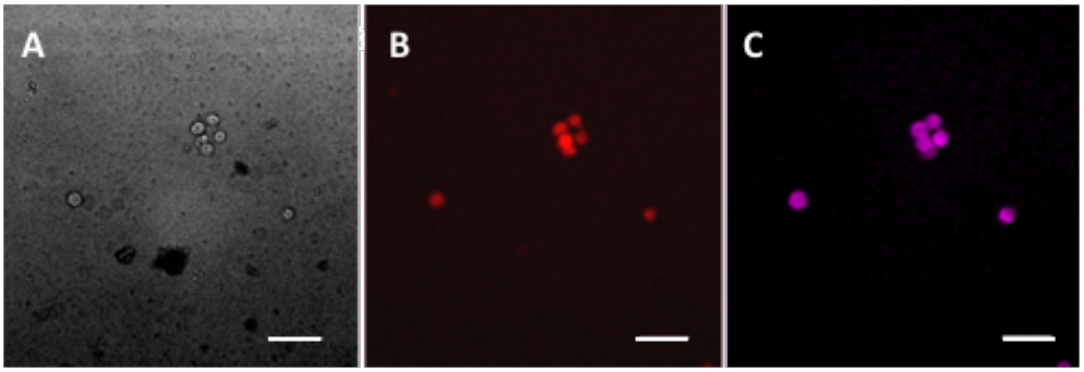
A
B
C

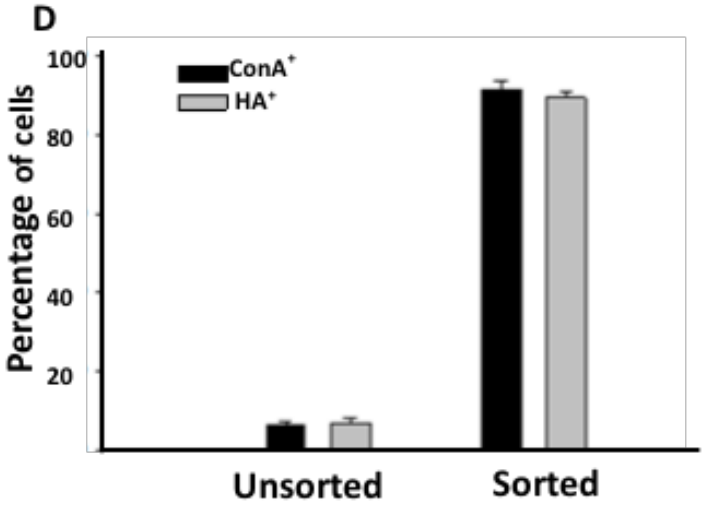
D
Percentage of cells
100
80
60
40
20
ConA+
HA+
Unsorted
Sorted

Figure 3.7. Representative microscopy images of HR cells isolated from a suspension of dissociated cells of 4 dpf zebrafish larvae (*Danio rerio*) obtained by fluorescence-activated cell sorting (FACS). (A-C) Transmitted light (A) or fluorescence microscopy images illustrating the co-localization of $ConA^+$ (B) and (C) H^+-$ATPase^+$ (C) cells isolated by FACS. Stained and unstained cells were counted and the percentage of HR cells in both the total and post-sort cell populations was determined (D). Data are presented as means ± standard error of the mean (SEM). Student's t-test, $P < 0.05$; N = 9 individual sorts is performed. Scale bars represent 50 µm

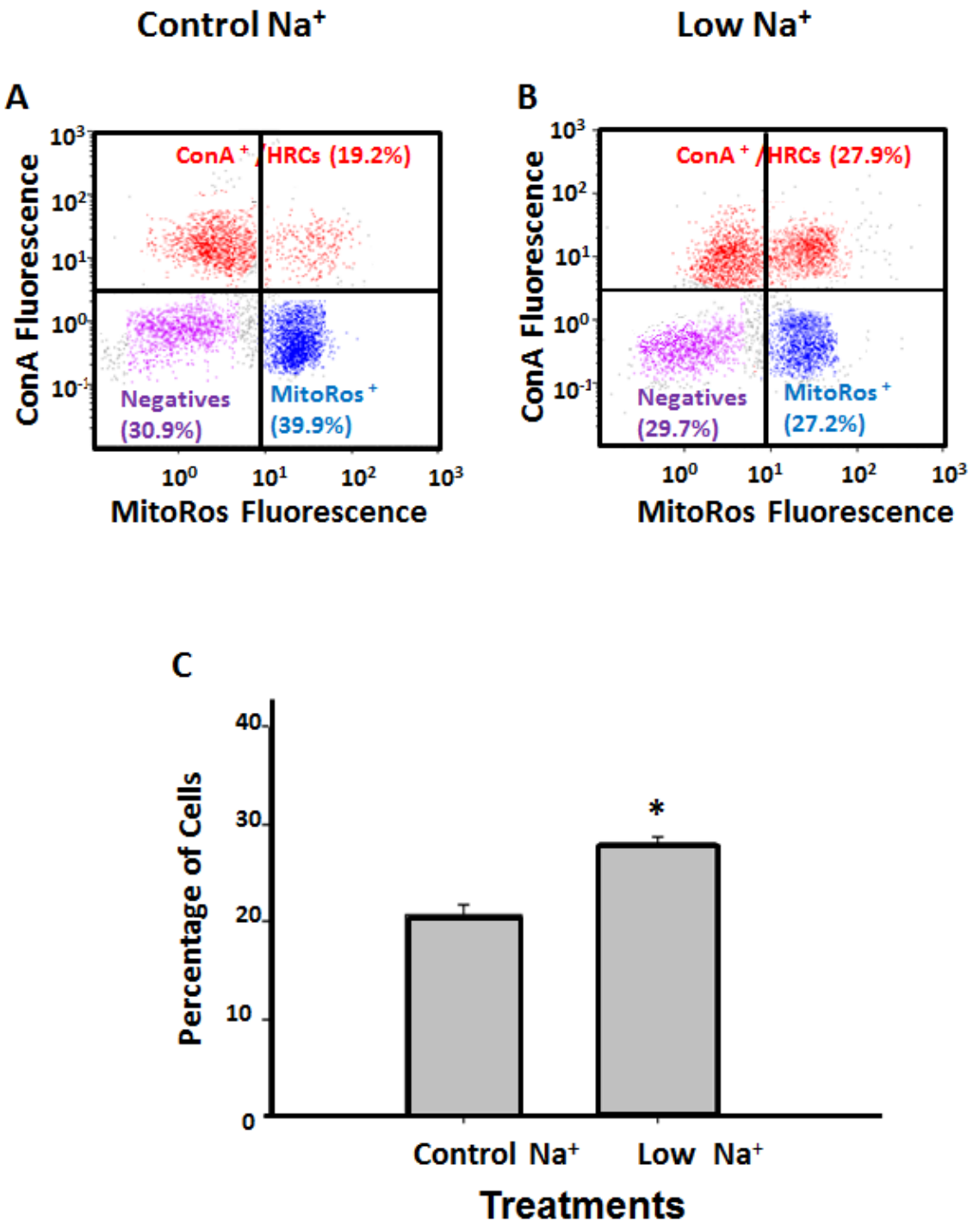
Control Na+
Low Na+
A
B
ConA Fluorescence
MitoRos Fluorescence
ConA+/HRCs (19.2%)
Negatives (30.9%)
MitoRos+ (39.9%)
ConA+/HRCs (27.9%)
Negatives (29.7%)
MitoRos+ (27.2%)
C
Percentage of Cells
*
Control Na+
Low Na+
Treatments

Figure 3.8. Representative flow cytometry data illustrating the percentage of ConA positive HR cells isolated from a 4 dpf zebrafish larvae (*Danio rerio*) dissociated cell suspension in control (800 µm) versus low Na^+ (5 µm) treatments. (A-B) The scatter plot flow cytometry data with X axis represent the fluorescence associates with MitoRos-labelled cells while the Y axis accounts for cells with ConA labled cells for the entire cell population (ConA positive cells indicated in red, MitoRos positive cells indicated in blue, and negative cells that exhibit no labelling of ConA or MitoRos indicated in purple). Fluorescence detected for ConA-labelled cells in control sodium water (19.2%) and low Na^+(B) (27.9%). (C)The percenage of $ConA^+$ cells (HR cells) in total isolated cells from 4 dpf zebrafish larvae compared between control Na^+ (800 µm) versus low Na^+ (5 µm)) treatments groups ·All data are presented as means +/- 1 SEM. An asterisk indicates a significant difference between groups (Student t-test, $P < 0.05$, $N = 8$).

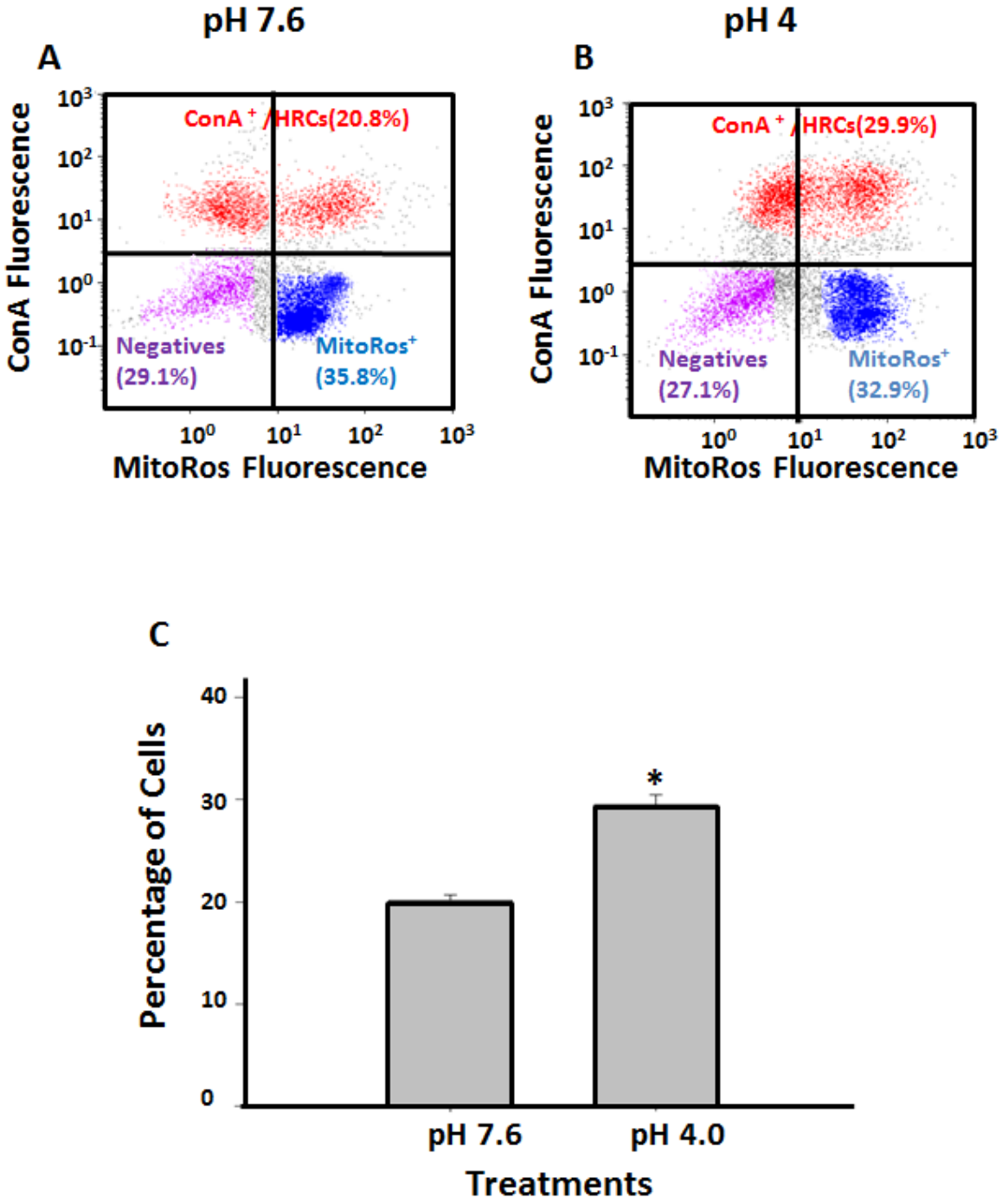
pH 7.6
A
ConA Fluorescence
ConA⁺ /HRCs(20.8%)
Negatives
(29.1%)
MitoRos⁺
(35.8%)
MitoRos Fluorescence
pH 4
B
ConA Fluorescence
ConA⁺ /HRCs(29.9%)
Negatives
(27.1%)
MitoRos⁺
(32.9%)
MitoRos Fluorescence
C
Percentage of Cells
pH 7.6
pH 4.0
Treatments

Figure 3.9. Representative flow cytometry data illustrating the percentage of ConA positive HR cells isolated from a 4 dpf zebrafish larvae (*Danio rerio*) dissociated cell suspension in control (pH 7.6) versus low pH (pH 4) treatments. (A&C):The dot plot flow cytometry data with X axis represent the fluorescence associates with MitoRos-labelled cells while the Y axis accounts for cells with ConA labbled cells for the entire cell population (ConA positive cells indicated in red, MitoRos positive cells indicated in blue, and negative cells that exhibit no labelling of exhibiting fluorescence associated with ConA labelling respectively. Fluorescence detected for ConA-labelled cells in control (A) (pH 7.6) versus low pH (B)(pH 4) treatments with 20.8% and 29.9% of the cells. (C)The percentage of ConA cells (HR cells) in total isolated cells from 4dpf zebrafish larvae compared between control pH (pH: 7.6) and low pH (pH:4) treatment groups. . All data are represented in mean +/- SEM. An asterisk indicates a significant difference between groups (Student t-test, $P < 0.05$, $N = 8$).

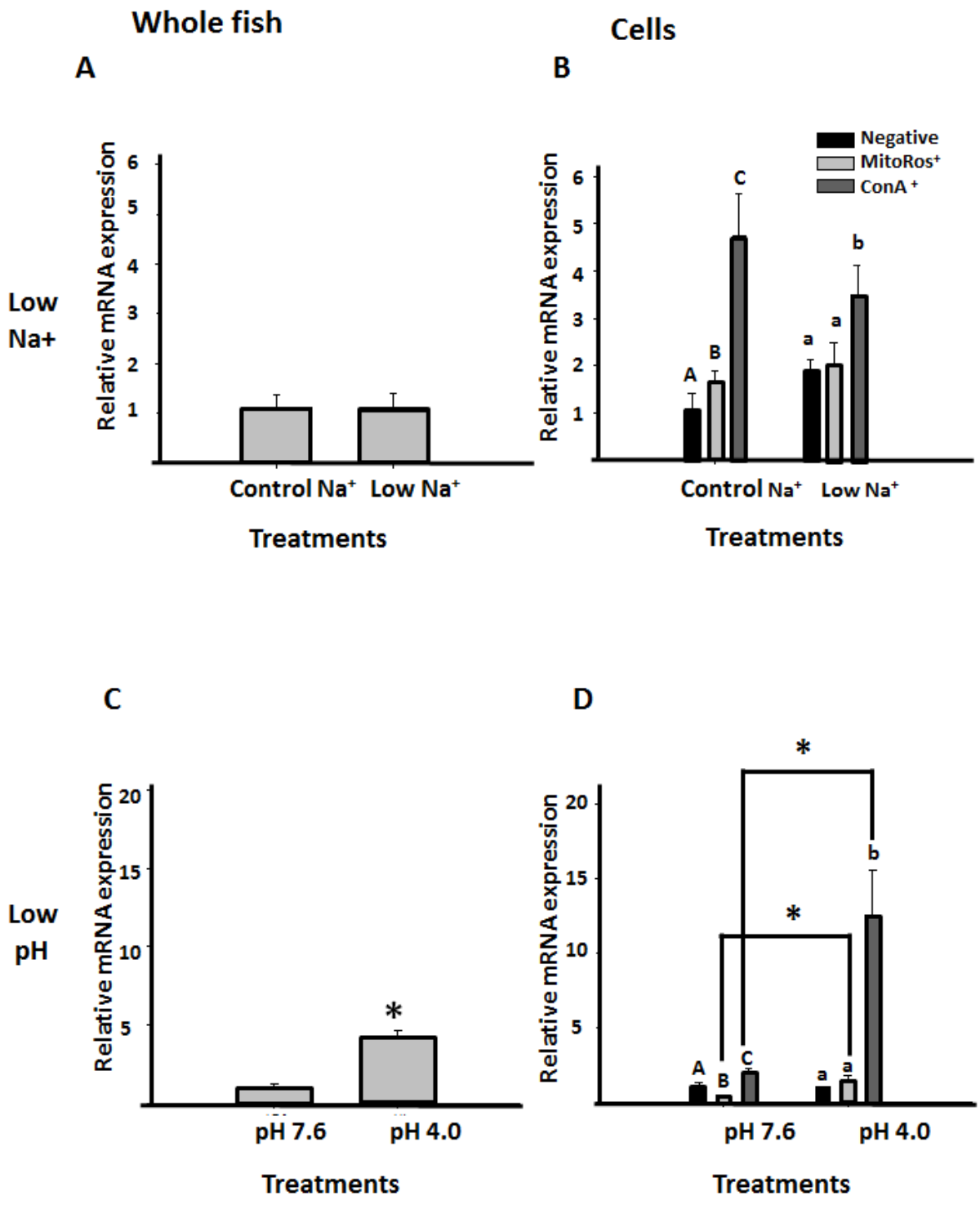
Whole fish
Cells
A
B
Low Na+
Relative mRNA expression
Negative
MitoRos+
ConA +
Control Na+
Low Na+
Treatments
C
D
Low pH
pH 7.6
pH 4.0
Treatments

Figure 3.10. The effects of low Na^+ or low pH exposure on relative mRNA levels of H^+-ATPase *(atpv61aa: NM_201135.2*) in whole zebrafish (*Danio rerio*) larvae at 4 dpf and three populations of sorted (FACS) cells obtained from the same pool of larvae. The *h^+-atpase* expression levels determined from mRNA obtained using whole fish (A, C) or isolated cell populations [HR cells, non-HR ionocytes and non-ionocytes (negatives)] (B, D) were compared in fish reared in normal Na^+ water (800 µm) versus low Na^+ (5 µm) water (A, B) and control pH (7.6) versus low pH (4.0) treatments (C, D). Data are presented as means ± 1 standard error of the mean (SEM). An asterisk indicates a significant difference between control and experimental groups. Whole larvae samples were analysed by one-way ANOVA followed by Holm-Sidak post-hoc test (N = 6). Isolated cells were analysed by two-way ANOVA followed by Holm-Sidak post-hoc test (N = 6). Within each group, means that do not share letters are statistically different and P-values of < 0.05 are considered significant.

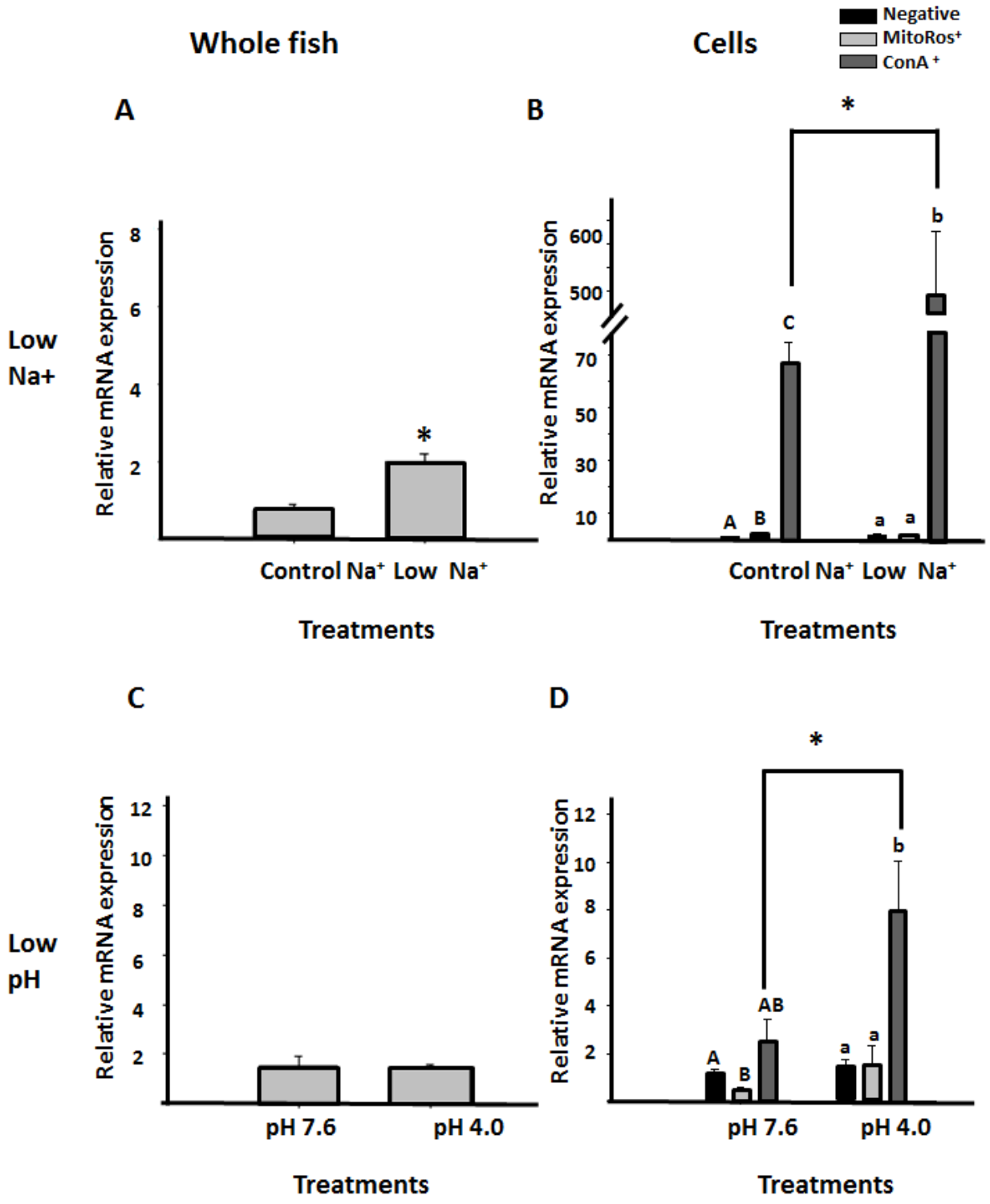
Whole fish
Cells
Negative
MitoRos+
ConA +
A
B
C
D
Low
Na+
Low
pH
Relative mRNA expression
Control Na+ Low Na+
pH 7.6
pH 4.0
Treatments
*
a
b
c
A
B
AB

Figure 3.11. The effects of low Na^+ or low pH exposure on relative mRNA levels of NHE3b *(slc9a3.2: XM_021468124.1)* in whole zebrafish (*Danio rerio*) larvae at 4 dpf and three populations of sorted (FACS) cells obtained from the same pool of larvae. The *nhe3b* expression levels determined from mRNA obtained using whole fish (A, C) or isolated cell populations [HR cells, non-HR ionocytes and non-ionocytes (negatives)] (B, D) were compared in fish reared in normal Na^+ water (800 µm) versus low Na^+ (5 µm) water (A, B) and control pH (7.6) versus low pH (4.0) treatments (C, D). Data are presented as means ± 1 standard error of the mean (SEM). An asterisk indicates a significant difference between control and experimental groups. Whole larvae samples were analysed by one-way ANOVA followed by Holm-Sidak post-hoc test (N = 6). Isolated cells were analysed by two-way ANOVA followed by Holm-Sidak post-hoc test (N = 6). Within each group, means that do not share letters are statistically different and P-values of < 0.05 are considered significant.

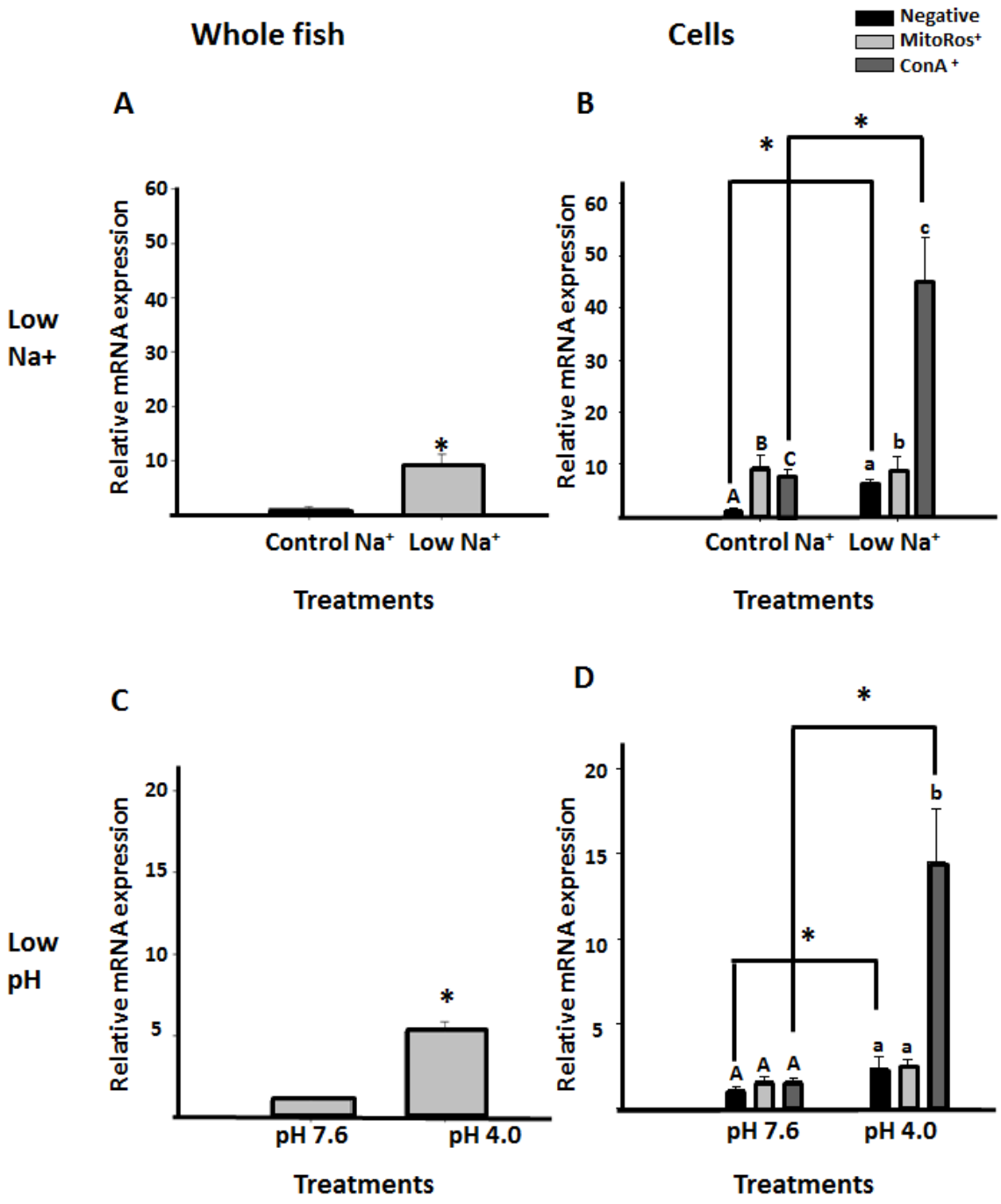
Whole fish
Cells
Negative
MitoRos+
ConA +
A
B
C
D
Low
Na+
Low
pH
Relative mRNA expression
Control Na+
Low Na+
pH 7.6
pH 4.0
Treatments
*
a
b
c
A
B
C

Figure 3.12. The effects of low Na^+ or low pH exposure on relative mRNA levels of Rh family, C glycoprotein b *(rhcgb: NM_017354103.2*) in whole zebrafish (*Danio rerio*) larvae at 4 dpf and three populations of sorted (FACS) cells obtained from the same pool of larvae. The *rhcgb* expression levels determined from mRNA obtained using whole fish (A,C) or isolated cell populations [HR cells, non-HR ionocytes and non-ionocytes (negatives)] (B,D) were compared in fish reared in normal Na^+ water (800 µm) versus low Na^+ (5 µm) water (A,B) and control pH (7.6) versus low pH (4.0) treatments (C,D). Data are presented as means ± 1 standard error of the mean (SEM). An asterisk indicates a significant difference between control and experimental groups. Whole larvae samples were analysed by one-way ANOVA followed by Holm-Sidak post-hoc test (N = 6). Isolated cells were analysed by two-way ANOVA followed by Holm-Sidak post-hoc test (N = 6). Within each group, means that do not share letters represent statistical differences and P-values of < 0.05 are considered significant.

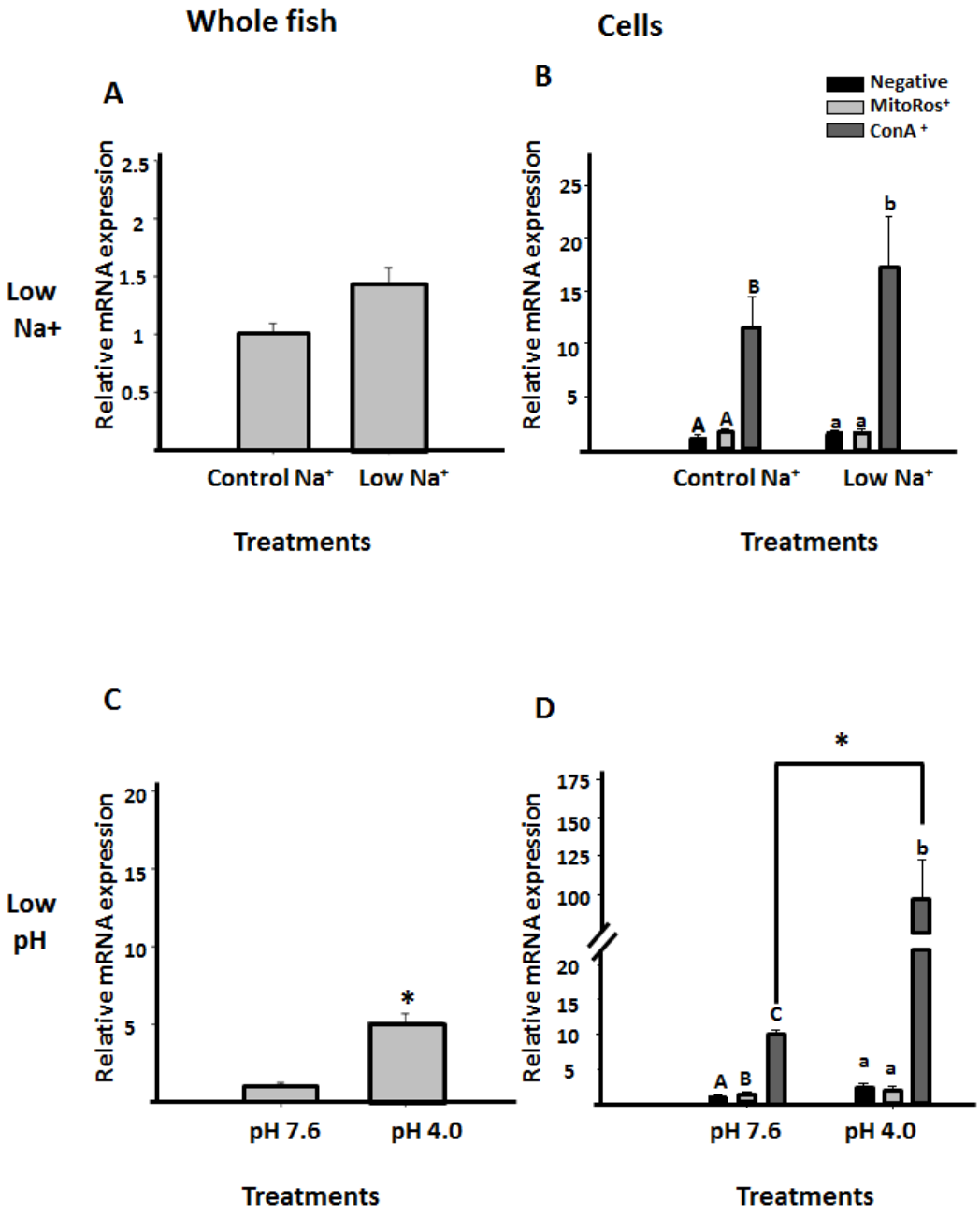
Whole fish
Cells
A
B
Negative
MitoRos+
ConA +
Low Na+
Relative mRNA expression
2.5
2
1.5
1
0.5
25
20
15
10
5
A
A
B
a
a
b
Control Na+
Low Na+
Treatments
C
D
Low pH
20
15
10
5
*
175
150
125
100
c
pH 7.6
pH 4.0

Figure 3.13. The effects of low Na^+ or low pH exposure on relative mRNA levels of carbonic anhydrase 15a *(ca15a: XM_017358460)* in whole zebrafish (*Danio rerio*) larvae at 4 dpf and three populations of sorted (FACS) cells obtained from the same pool of larvae. The *ca15a* expression levels determined from mRNA obtained using whole fish (A,C) or isolated cell populations [HR cells, non-HR ionocytes and non-ionocytes (negatives)] (B,D) were compared in fish reared in normal Na^+ water (800 µm) versus low Na^+ (5 µm) water (A,B) and control pH (7.6) versus low pH (4.0) treatments (C,D). Data are presented as means ± 1 standard error of the mean (SEM). An asterisk indicates a significant difference between control and experimental groups. Whole larvae samples were analysed by one-way ANOVA followed by Holm-Sidak post-hoc test (N = 6). Isolated cells were analysed by two-way ANOVA followed by Holm-Sidak post-hoc test (N = 6) and P-values of < 0.05 are considered significant.

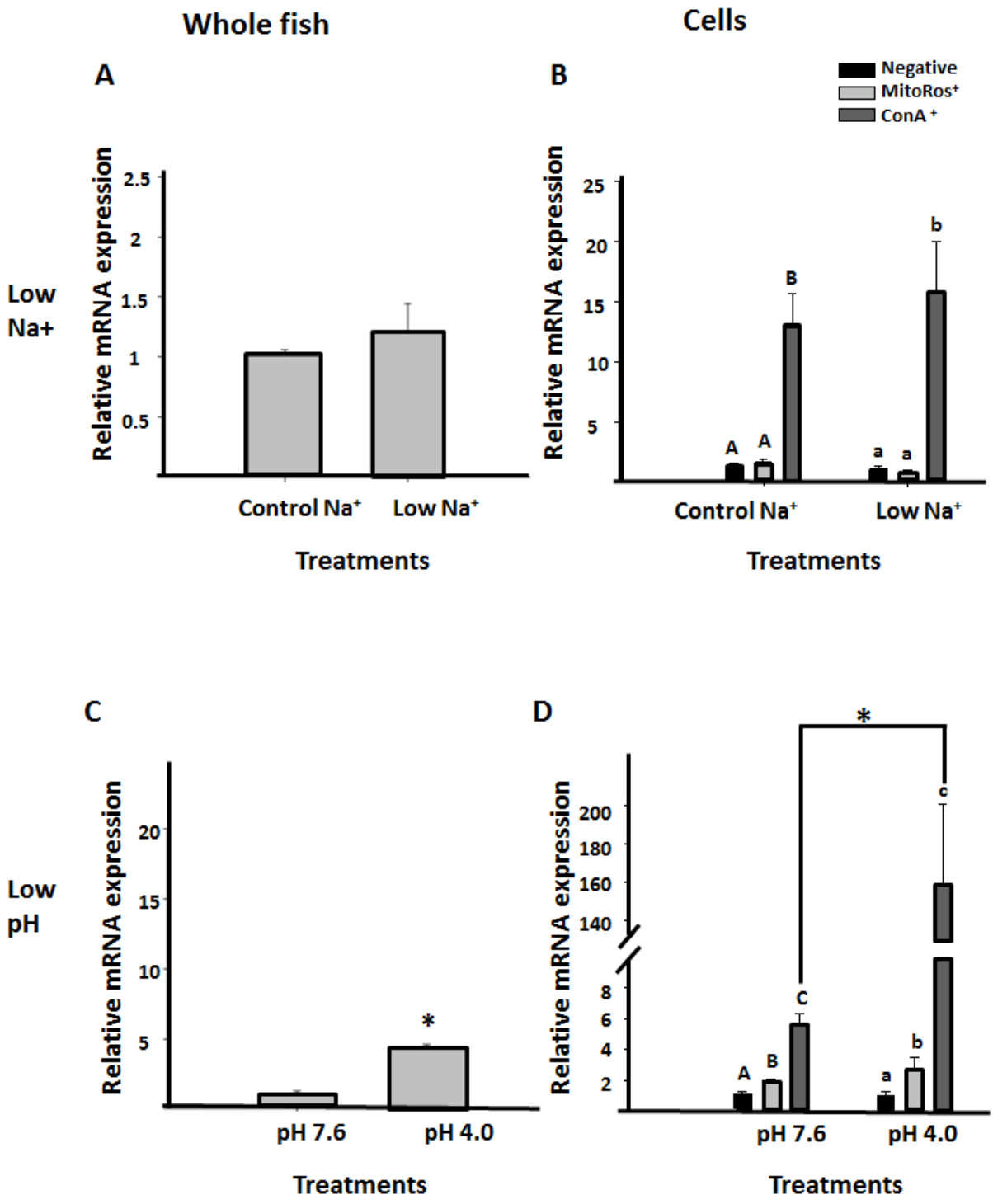
Whole fish
Cells
A
B
Negative
MitoRos+
ConA +
Low Na+
Relative mRNA expression
2.5
2
1.5
1
0.5
25
20
15
10
5
A
A
B
a
a
b
Control Na+
Low Na+
Treatments
C
D
Low pH
20
15
10
5
200
180
160
140
8
6
4
2
*
c
C
b
pH 7.6
pH 4.0

Figure 3.14. The effects of low Na^+ or low pH exposure on relative mRNA levels of carbonic anhydrase 17a *(ca17a: NM_ BC057412*) in whole zebrafish (*Danio rerio*) larvae at 4 dpf and three populations of sorted (FACS) cells obtained from the same pool of larvae. The *ca17a* expression levels determined from mRNA obtained using whole fish (A,C) or isolated cell populations [HR cells, non-HR ionocytes and non-ionocytes (negatives)] (B,D) were compared in fish reared in normal Na^+ water (800 µm) versus low Na^+ (5 µm) water (A,B) and control pH (7.6) versus low pH (4.0) treatments (C,D). Data are presented as means ± 1 standard error of the mean (SEM). An asterisk indicates a significant difference between control and experimental groups. Whole larvae samples were analysed by one-way ANOVA followed by Holm-Sidak post-hoc test (N = 6). Isolated cells were analysed by two-way ANOVA followed by Holm-Sidak post-hoc test (N = 6). Within each group, means that do not share letters represent statistical differences and P-values of < 0.05 are considered significant.

Discussion

In this thesis, I developed and validated a method based on FACS to isolate for the first-time specific populations of living ionocytes from zebrafish larvae. The technique enabled subsequent analyses of gene (mRNA) expression in three groups of cells; an enriched pool of HR cells, a mixed population of all other (non-HR cell) mitochondrion-rich ionocytes and an assortment of negative (non-ionocyte) cells. Three major findings emerged from this thesis;

1. Consistent with current models of HR cell function in zebrafish larvae (e.g. Fig. 1 in Guh et al., 2015), the mRNA levels of five genes thought to be involved in HR cell Na^+ uptake and H^+ secretion (*h^+-atpase*, *nhe3b*, *rhcgb, ca15a, ca17a)* generally were enriched markedly in the HR cells relative to the other ionocytes and non-ionocytes (negative cells).
2. Environmental acclimation of zebrafish larvae to water of low Na^+ content or low pH elicited changes in gene expression in HR cells that typically were of a larger magnitude than in whole larvae. These results demonstrate an advantage of cell-specific versus whole larva mRNA analyses.
3. The increases in gene expression in larvae exposed to low Na^+ or acidic water were the combined result of increased numbers of HR cells and importantly, **HR cell-specific** increases in mRNA expression, of the five genes being studied.

Overall, the results of this thesis demonstrate that the isolation and analyses of living ionocytes, while labour- and time-intensive, allows for a more accurate assessment of ionocyte-specific mRNA levels of genes of interest compared to the traditional analysis of whole larva gene expression. Using this approach, this study arguably provides the most convincing gene expression data to date supporting proposed models of HR cell responses to low ambient Na^+ levels and acidic water.

Isolation of ionocyte subtypes – the pros and cons.

The focus of this thesis was the HR ionocyte subtype owing to the wealth of existing data surrounding its proposed involvement in acid-base regulation and Na^+ uptake and its straightforward identification using the fluorescently-tagged vital HR cell marker, ConA. The use of FACS requires that the cells of interest be labelled and present within a suspension of dissociated cells. Thus, an initial focus of the study was to specifically label HR cells of zebrafish larvae and generate a pool of labelled and unlabelled dissociated cells for subsequent analysis of cell-specific mRNA levels. In my thesis, ConA was used to distinguish HR cells from the other cell populations in larvae. Horng et al. (2007) first reported that ConA bound to a specific population of cells in the skin of zebrafish larvae that were enriched with H^+-ATPase (HA) and thus deemed to be HR ionocytes. Therefore, an important initial experiment in the current study was to use an HR cell-specific HA antibody in combination with ConA in whole fish and isolated cells to determine the specificity of ConA as a marker for HR cells in my specific application. Furthermore, it was demonstrated by microscopy and flow cytometry that non-specific binding of ConA did not occur in dissociated cell populations before or after sorting. A second advantage of labelling cells with ConA is that it permits the isolation of live cells, which facilitates RNA extraction (albeit RNA

degradation can be a problem) compared to cells fixed with paraformaldehyde whereby cross-linking of protein and RNA hinders RNA extraction (David et al., 2011). Using ConA in combination with the mitochondrial stain, MitoRos, also allowed for the isolation of a non-HR cell pool of ionocytes, a mixed population of $ConA^-/MitoRos^+$ NaR and NCC cells. Finally, a third population of remaining cells (non-ionocytes) could be sorted simultaneously as a $ConA^-/MitoRos^-$ fraction.

In the current study, not all of the sorted HR cells were $MitoRos^+$. Indeed typically, there was a significant fraction of $ConA^+$ cells that were categorised as $MitoRos^-$ during FACS. However, although MitoRos staining of these cells was below the threshold set for FACS detection, they nevertheless did exhibit a low level of MitoRos staining when examined by IHC. Thus, the final population of HR cells that was examined for gene expression was a mixture of cells exhibiting a gradient of MitoRos staining. In all cases, however, the cells co-expressed ConA and HA. The variability in the intensity of MitoRos staining of HR cells suggests that these cells may represent different developmental stages or indeed distinct sub-types of HR cells. Thus, it would be informative in future studies to compare target gene mRNA levels in two sorted populations of HR cells exhibiting extremes in MitoRos staining. In contrast to the HR cells, the NaR and NCC cells did not appear to exhibit a gradient of MitoRos staining when viewed after IHC. Therefore, it is unlikely that the final population of non-HR cell ionocytes that were sorted on the basis of MitoRos fluorescence intensity was underrepresenting the *in vivo* numbers of NaR and NCC cells.

One of the major concerns related to analysis of mRNA obtained from whole larvae in studies evaluating ionic or acid-base regulation is that ionocytes are massively underrepresented in comparison to total cells (e.g. ~400 HR cells per fish in comparison to millions of other cells), making it challenging to detect subtle changes in gene expression that may be specific to HR cells

or other ionocytes. In the present study, the fraction of ConA^{+} HR cells sorted by FACS (~17-25%) clearly was higher than *in vivo*. The increase in the relative proportion of HR cells was the result of several factors including removal of cellular debris from total cells by centrifugation prior to sorting and by exclusion of debris, dead cells, clumps of cells or doublets by sorting from a pre-selected region that excluded those events during FACS (Appendix 1). Although, cell sorting occurred in multiple episodes, numbers of HR cells were kept the same (300,000 HR cells) for each sort and the total mRNA level for each sort was also kept constant. In summary, FACS using ConA and MitoRos is a viable method for isolating highly enriched populations of HR cells and non-HR ionocytes from zebrafish larvae. The main advantage of this approach is that it increases the probability of detecting changes in cell-specific gene expression that otherwise might be undetectable using whole larva homogenates. In addition, any changes in mRNA that are detected can be evaluated as potentially biologically relevant rather than being treated as simply statistically significant differences that may convey little biological meaning.

However, there are some shortcomings associated with cell sorting prior to gene expression analysis. Obviously, the procedure is laborious, time-consuming and can be expensive depending on the type of sorting facility being used (user fees). These disadvantages must be weighed against the potential benefits of cell sorting. Another possible negative outcome of cell sorting is that changes in mRNA levels incurred *in vivo* may be reversed upon removal of the environmental stimulus. In addition to natural mRNA turnover tending to lower levels during sorting, there is a greater potential for RNA degradation by non-endogenous RNAse and contamination from exogenous templates.

Responses of HR cells to low environmental Na^+

It has long been known that acclimation (or adaptation) of fish to waters of low Na^+ content elicits compensatory responses aimed at maintaining normal rates of Na^+ uptake in the face of reduced Na^+ availability (Boisen et al., 2003; Laurent and Perry, 1991; McDonald and Rogano, 1986; Perry and Laurent, 1989). In zebrafish, arguably the most significant compensatory response to low ambient Na^+, is an enhanced ability to absorb Na^+ owing to increases in both Na^+ uptake affinity and capacity (Boisen et al., 2003).Thus, Na^+ uptake is preserved partially by the increase in the affinity of Na^+ uptake (Boisen et al., 2003) and increased markedly upon return to normal ambient Na^+ levels because of the elevated uptake capacity (Boisen et al., 2003; Kumai et al., 2012; Kwong et al., 2014). It has been suggested that the predominant pathway enabling Na^+ uptake in zebrafish larvae exposed to low Na^+ water is via NHE3b linked to ammonia excretion through Rhcgb (Shih et al., 2012). In agreement with the proposed metabolon model of Wright and Wood (Wright and Wood, 2009) that was verified recently (Ito et al., 2013), the close association of NHE3b, Rhcgb and CA17a facilitates Na^+ uptake and ammonia excretion by promoting chemical gradients favouring Na^+/H^+ exchange and NH_3 diffusion. Specifically, $[H^+]$ in the external boundary layer is lowered by the protonation of NH_3 to NH_4^+. While the lowering of $[H^+]$ facilitates Na^+/H^+ exchange, the chemical removal of NH_3 (by its conversion to NH_4^+) serves to sustain NH_3 diffusion gradients. The role of CA17a is to provide a source of intracellular H^+ in close proximity to NHE3b to fuel the exchanger. Accordingly, one would predict HR cell-specific increases in mRNA expression of *nhe3b*, *rhcgb* and *ca17a* in fish exposed to low environmental Na^+. In the current study, however, only *nhe3b* and *rhcgb* were increased by 7-fold and 4.2-fold, respectively (table 4.3); *ca17a* levels were unchanged. Statistically significant increases in *nhe3b*

and *rhcgb* also were detected using whole larvae although for *nhe3b*, the magnitude of the mRNA increase was smaller in comparison to the HR cell-specific increases. Only two other studies have reported mRNA levels for one or both of these genes in zebrafish larvae acclimated to low Na^+. Shih et al. (Shih et al., 2012) measured a small (1.5-fold) increase in *nhe3b* levels in whole larvae while *rhcgb* expression was unaltered. In the study of Nakada et al. (2007), a single representative western blot image depicts an apparent increase in Rhcgb protein in 6 dpf larvae acclimated to 1/20X FW. In adult zebrafish gill, *nhe3b* was increased by 1.6- to 2.6-fold in fish acclimated to water of low Na^+ content (Shih et al., 2012; Yan et al., 2007) and *rhcgb* was elevated approximately 1.7-fold (Shih et al., 2012). The changes in mRNA expression of these genes in adult gill presumably reflect the combined actions of HR-specific modifications coupled with any possible increases in the numbers of HR cells associated with low-Na^+ acclimation. The data from Ito et al. (2013) indicated that the expression of *ca17a* in 7 dpf larvae exposed to low Na^+ water was increased. However, Lin et al. (2008) reported stable levels of *ca17a* in gills of adult zebrafish acclimated to low environmental Na^+.

The increases in gene expression of *nhe3b* and *rhcgb* reported here are consistent with the metabolon model of Na^+ uptake that is known to operate in zebrafish larvae under conditions of low ambient Na^+ (Shih et al., 2012). However, the lack of an increase in HR cell-specific expression of *ca17a* was unexpected. For NHE3b to continue to function at low external levels of Na^+, the H^+ gradient across the HR cell apical membrane must increase through the combined actions of extracellular alkalization (via Rhcgb) and intracellular acidification. Thus, it was expected that c*a17a* levels would increase to facilitate an increase in H^+ production from the

catalysed hydration of CO_2. It is possible that intracellular CA activity was increased despite constant mRNA levels owing to post-translational modifications (Carrie and Gilmour, 2016).

In addition to the HR cell-specific increases in gene expression reported in this study, any changes in whole larva mRNA levels will also reflect the increased numbers of HR cells especially for genes such as *nhe3b* that are highly enriched within the HR cell. The flow cytometry data presented in the current study indicated a significantly higher percentage of HR cells isolated from zebrafish larvae exposed to low Na^+ (27.9%) compared to those exposed to control water (19.2%).

Previous studies have documented that *atpv6v1aa* mRNA levels are lowered in whole larvae (Shih et al., 2012) or adult gill (Shih et al., 2012; Yan et al., 2007) during acclimation of fish to low Na^+ water. It was argued that a decrease in HR cell HA activity would benefit NHE3b function in low Na^+ water by the presumed resultant increase in cytosolic H^+ activity. In this thesis, there was no effect of acclimation to low Na^+ on HR cell-specific *atpv6v1aa* amounts although there was an apparent trend for lowered levels ($P = 0.097$). Similarly, *atpv6v1aa* levels assessed in whole larvae were unaffected by low Na^+ acclimation despite the greater numbers of HR cells known to be enriched in *atpv6v1aa*. The constancy of *atpv6v1aa* in the face of HR cell proliferation, is in itself, indirect evidence for a decline in HR cell *atpv6v1aa* levels.

The role of CA15a in HR cell-mediated Na^+ uptake, ammonia excretion and acid-base balance is not well understood. Although it is agreed that CA15a is positioned to catalyse boundary layer reactions involving CO_2/HCO_3^- owing to its anchorage to the apical membrane of HR cells (Lin et al., 2008) or other acid-secreting ionocytes (Wright and Wood, 2009) there is some debate as to whether it catalyses dehydration or hydration reactions. According to Lin et al.

(2008), apically oriented CA15a catalyses the dehydration of HCO_3^-, which serves to increase boundary layer pH and thus facilitate NHE3b function by increasing the transepithelial H^+ gradient [see Fig. 1 in Guh et al. (2015)]. On the other hand, Wright and Wood (2009) suggested that apical CA (termed CAIV in their model), catalyses the hydration of CO_2 to generate H^+ in the boundary layer to assist ammonia excretion via acid-trapping (Wright et al., 1989). Regardless of which model is correct, *ca15a* expression was unchanged by low Na^+ treatment in the present study although there was an apparent trend for increased mRNA levels in whole larvae and HR cells. Thus, unlike in the adult zebrafish gill, which exhibits an increase in *ca15a* during low Na^+ exposure (Ito et al., 2013; Lin et al., 2008), Na^+ uptake by the larval HR cell under similar conditions may not be regulated in the same fashion.

In summary, the current data reinforce the view that NHE3b (functioning in association with Rhcgb) is the dominant ion transport protein maintaining Na^+ homeostasis in fish acclimated to low environmental Na^+ (Shih et al., 2012; Horng et al., 2009; Kumai and Perry, 2011). Furthermore, the results of this thesis suggest that the HR cell proliferation in addition to HR-specific transcriptional control are both involved in the acclimation responses to low-Na^+ environmental conditions.

Responses of HR cells to low environmental pH

Like in many other species, exposure of zebrafish to acidic water causes a transient reduction in whole body Na^+ levels (Kumai et al., 2011). In zebrafish, the recovery of whole body Na^+ content is the result of a stimulation of Na^+ uptake in the face of persistently elevated Na^+ efflux (Kumai et al., 2011). The ability of zebrafish to elevate Na^+ uptake apparently is a unique

strategy among fresh water teleosts to restore Na^+ balance during exposure to acidic water (Kwong et al., 2014).

Although it is generally assumed that exposure of zebrafish to acidic water elicits metabolic acidosis (Lin et al., 2005), there are no actual data to support this view. In other fish species, the effects of water acidification on blood acid-base status is dependent upon water hardness (Ca^{2+} levels); in soft water, external acidification elicits ionic disturbances without affecting blood acid-base balance whereas in hard water, metabolic acidosis develops with no change in plasma ion levels (see review by Kwong et al., 2014). In the present study, the water more closely resembled hard water ($[Ca^{2+}]$ = 0.25 mM) and certainly did not contain the very low levels of Ca^{2+} known to be associated with metabolic acidosis upon external acidification. Thus, in this thesis I have assumed that exposure of zebrafish larvae to acidic water disrupted both Na^+ and H^+ balance. Therefore, this thesis focused on quantifying the numbers of HR cells and the HR cell-specific genes thought to be involved in Na^+ uptake and H^+ secretion in an attempt to gain additional insight into potential mechanisms underlying the increase in Na^+ uptake and presumed H^+ secretion in fish exposed to water of low pH.

An increase in HR cell density was documented previously as a key physiological response to acid exposure in zebrafish larvae and adult gill (Chang et al., 2009; Horng et al., 2009). In the current study, the flow cytometry data are consistent with these previous studies, with a significantly larger percentage of HR cells isolated from zebrafish larvae exposed to low pH (~29%) as compared to control larvae (~20%). Taken together, these results suggest that as a compensatory response to exposure to acidic water, zebrafish larvae undergo a proliferation of HR cells on epithelial surfaces. Importantly, the results indicate that when relying on tissue or

whole-body analyses, any changes in mRNA expression of genes localised to HR cells will be the result of increased HR cell numbers coupled with any HR cell-specific changes in gene expression.

Several studies have investigated the effects of low ambient pH on gene expression in zebrafish larvae and adult gill; the results of these previous experiments are summarised in Table 4.1. Two important findings emerge from these data; first, depending on the gene being evaluated, the results can vary markedly between studies, and second, the effects of external acidification on mRNA levels can differ when comparing data from adult gill and whole larvae. As pointed out by Lin et al. (2015), a possible explanation for the differences when comparing gills and larvae is that whole larvae likely express ion transport genes at numerous locations other than the ionocytes of the yolk sac epithelium, including the kidney and intestine. Differences in results between studies, even when assessing equivalent tissues (i.e. gill or whole larvae), might also arise from variability in the proportion of target cells (e.g. HR cells) in the mixed population of cells extracted from the target tissues. By assessing mRNA levels with and without FACS, the results of this thesis provide the first data on HR cell-specific changes in gene expression in zebrafish larvae exposed to acidic water, which are compared with data obtained from whole larvae.

Kumai et al. (2011) presented compelling evidence to support a more important role for NHE3b in Na^+ uptake in zebrafish larvae reared in acidic water compared to neutral water. However, despite the prediction of increased *nhe3b* expression, mRNA levels were unchanged in acidic larvae, a result that was attributed to the possible "masking" of HR cell-specific changes by a lack of any changes (or opposing changes) in *nhe3b* expression in the non-HR cells (Kumai et al., 2011). Indeed, the results of this thesis support their interpretation; *nhe3b* levels were

unchanged in whole larvae but were increased approximately 4-fold in HR cells (Table 4.4). Thus, the finding of reduced *nhe3b* levels in gill from adults exposed to acidic water (Yan et al., 2007; Chang et al., 2013), should be interpreted with caution until comparable data are obtained from HR cells sorted from adult gill.

The increased significance of NHE3b to Na^+ uptake in zebrafish exposed to acidic water reflects its reliance on the HR cell metabolon (Ito et al., 2013) whereby Na^+ uptake is facilitated by the concerted effects of increased ammonia excretion via Rhcgb and increasing intracellular H^+ availability via CA. The results of this study demonstrating higher levels of *rhcgb* and *ca17a* specifically in HR cells add increasing support to the model of Na^+ uptake in acidic water (Kumai et al., 2011) whereby increasing ammonia excretion (as NH_3) serves to increase boundary layer pH while an increase in cytosolic CA activity causes intracellular acidification. Ultimately, both of these factors contribute to increasing Na^+ uptake via NHE3b by increasing the H^+ gradient across the HR cell apical membrane. Kumai et al. (2011) also suggested that the metabolon model of Na^+ uptake in acidic water was being assisted by an increasing contribution of HA-mediated H^+ excretion, which serves to enhance NH_3 diffusion. The increased mRNA expression of *atpv6v1aa* in HR cells in larvae exposed to water of low pH is consistent with its purported role in Na^+ uptake. Moreover, the occurrence of this response supports the notion of the HR cell as the main acid/base regulating cell in zebrafish larvae (Horng et al., 2007; Horng et al., 2009; Hwang et al., 2011). Interestingly, the non-ionocyte population exhibited a significant increase in *rhcgb* when larvae were exposed to acidic water. It is important to recognize that the non-ionocytes fraction presumably included cells from other tissues that could also be important for acid base regulation and Na^+ uptake (e.g. Nawata et al., 2007).

Similar to previous studies on larvae or gill (Lin et al., 2008; 2015), *ca15a* expression was increased by acidic water treatment in larvae or HR cells. Depending on whether CA15a is catalysing boundary layer hydration of dehydration reactions, its increased activity would promote NHE3b function either by lowering $[H^+]$ in the boundary layer (via dehydration of HCO_3^-) or providing a source of H^+ for NH_3 protonation (via hydration of CO_2); in either case, Na^+ uptake by NHE3b is expected to increase.

Conclusions and perspectives

Previous research efforts on the gill/skin of zebrafish revealed a complex network of regulatory responses accompanying low Na^+ and low pH which, have improved our understanding of fundamental ion transport mechanisms in HR cells (see Tables 4.1 and 4.2). The results of the current thesis extend this knowledge by providing the first data on HR cell-specific changes in gene expression as compensatory mechanisms to offset the deleterious effects of low Na^+ and low pH on ionocyte function. Specifically, this thesis demonstrates that the expression of several key target genes (*h^+-atpase*, *nhe3b*, *rhcgb, ca15a, ca17a)* is regulated in HR cells and that this regulation occurred independently of any changes in the number of HR cells.

The primary benefit of FACS is that cell-type specific mRNA data are generated, which can eliminate the confounding effects of mRNA changes in other cell types. Second, because multiple embryos (1000 zebrafish larvae) for each sort are usually processed to isolate cells, the effects of embryo-to-embryo variability are reduced. On the other hand, because HR cells are small population of total cells in zebrafish, sorting this population in high purity requires an excessive amount of time and labor.

Some genes that were previously proposed to control ion regulation in zebrafish have had their actions re-clarified by the current study into the precise pathways and target transporter/ionocytes in the zebrafish HR cell model. For instance, the results of this thesis indicate that the low pH treatment did not affect the *nhe3b* mRNA expression in whole larvae but at the cellular level this gene is upregulated. Furthermore, *h^+-atpase*, *rhcgb, ca15a* and *ca17* gene expression increased in whole larvae but to a much greater extent in HR cells when zebrafish are exposed to low pH. These results are consistent with Nakada et al. (2007) and Weiner et al. (2012) that Rhcbg and HA, NHE3b are functionally coupled in which both HA and NHE3b enable H^+ secretion and Rhcbg may drive the NHE3b by generating H^+ gradients across apical membranes of HR cells to perform acid/base regulation.

However, the result from low Na^+ treatment indicates an increase in *nhe3b*, and *rhcgb* with no changes in CA isoforms and *h^+-atpase* in both whole larvae and HR cells. These results suggest that CAs isoforms and other metabolons (i.e. NHE3b and Rhcgb,) are the key players by forming a closely associated complex to perform Na^+ uptake (Kumai et al., 2011; Nakada et al., 2007; Shih et al., 2012)

In conclusion, this study established an applicable technique to define the importance of cell specific responses to various environmental conditions (low pH and low Na^+) in zebrafish larvae. With this new technique, I was able to demonstrate HR cell-specific changes in gene expression associated with these harsh environmental conditions. Presumably the advantage of FACs will be cell-type specific and the decision on whether to pursue FACS as a technique to estimate cellular gene expression should carefully weigh the pros and cons.

Future studies

Using FACS to sort HR cells, we tentatively identified two sub-populations of HR cells that stain differently with MitoRos. These cells should be further analyzed separately to determine whether they are functionally different and respond differentially to varying environmental condition. In addition, the cells that stain with only MitoRos were identified as other types of ionocytes (NCC and NaR cells; Appendices 5 and 6). NCC cells in zebrafish were found to be involved in the compensatory regulation of Na^+ uptake following acid exposure (Chang et al 2013). Also, it is known that acid exposure increases the number of NaR cells due to an increase in cortisol levels. However, the mechanism(s) promoting the proliferation of NaR cells is not clearly understood (Kumai et al., 2012, Cruz et al., 2013). The use of FACS opens up new possibilities to study Na^+ uptake and acid-base regulatory mechanisms in other ionocyte subtypes to allow a more precise study of ion regulation in zebrafish.

One thing to note about the current study is it utilizes mRNA expression levels as a means of estimating functional differences that actually occur at the protein level. However, it is conceivable that mRNA expression differences may not reflect actual changes at the protein level within the cells. Therefore, future studies could be conducted to directly measure changes in protein levels within HR cells in response to exposure to low Na^+ and low pH environments. Furthermore, the combination of FACS with other high throughput techniques such as proteomics or transcriptomics may be useful to analyze total protein and transcript of larvae or adults to generate lists of mRNA and proteins expressed in each type of ionocytes individually.

These experiments will provide a better understating of possible differences in strategies of ion regulation in larvae and adults.

Another potential future experiment is to treat zebrafish larvae with hormones known to affect acid-base regulation and Na^+ uptake. One specific area worth investigating is to determine the effects of cortisol on gene and protein expression in zebrafish larvae HR cells. Recent studies have found that cortisol increases acid secretion and Na^+ uptake in zebrafish HR cells (Kumai and Perry, 2012; Lin et al., 2015). In addition, exposure to cortisol was found to increase the number of HR cells in zebrafish larvae by regulating a transcription factors required for the development of HR cells (Cruz et al., 2013). Furthermore, the expression of HA and NHE3b was upregulated in 1 dpf zebrafish embryos by cortisol treatment (Cruz et al., 2013). In contrast, exposure to cortisol for 48 h appeared to have a significant effect on CA expression levels in rainbow trout (Lin and Randall, 1993), but not on NHE3b expression levels in 4 dpf zebrafish larvae (Kumai and Perry, 2012). As such, while cortisol stimulates ionocyte proliferation in zebrafish larvae, its effects on gene expression do not appear to be consistent to those observed in larvae exposed to low-pH environments. The use of FACS can provide a comprehensive and integrated approach to elucidate the effects of cortisol on the expression of different genes in individual HR cells.

Table 4.1. A summary of previous studies showing the effects of low Na^+ or low pH exposure on the mRNA levels of selected ion transport genes in zebrafish gill and larvae

Ion transporter	Low Na^+	Low pH
h^+-atpase	Decreased in gill (Shih et al., 2012; Yan et al., 2007) Decreased in 4 dpf larvae (Shih et al., 2012)	Increased in gill (Yan et al., 2007) Increased in 3dpf larvae (Chang et al., 2009; Lin et al., 2015) No change in 3dpf larvae (Kwong and Perry, 2014)
nhe3b	Increased in gill (Shih et al., 2012, Yan et al., 2007) Increased in 4 dpf larvae (Shih et al., 2012)	Decreased in gill (Yan et al., 2007; Chang et al., 2013) Increased in 3dpf larvae (Lin et al., 2015) No change in 4dpf larvae (Kumai and Perry 2011)
rhcgb	Increased in gill (Shih et al., 2012) Increased in gill (Nakada et al., 2007) No change in 4 dpf larvae (Shih et al., 2012)	Increased in 3dpf larvae (Lin et al., 2015)
ca15a	Increased in gill (Lin et al., 2008)	Increased in gill (Lin et al., 2008)

	Increased in 7 dpf zebrafish larvae (Ito et al., 2013)	Increased in 3dpf larvae (Lin et al., 2015)
ca17a	No change in gill (Lin et al., 2008) Increased in 7 dpf zebrafish larvae (Ito et al., 2013)	Increased in 3dpf larvae (Lin et al., 2015) No change in gill (Lin et al., 2008)

Table 4.2. Effects of low Na^+ and low pH on the regulation of major ion transporters in zebrafish HR cells in present study

Ion transporters	Low-Na^+	Low-pH
h^+-atpase	No change	Increased
nhe3b	Increased	Increased
rhcgb	Increased	Increased
ca15a	No change	Increased
ca17a	No change	Increased

Table 4.3. Effects of low Na^+ on the regulation of major ion transporters in whole zebrafish larvae compared with HR cells in present study

Ion transporters	Whole fish (low- versus control-Na^+)	HR cells (low versus control-Na^+)
h^+-atpase	No change	No change
nhe3b	2-fold increase	7- fold increase
rhcgb	10-fold increase	4.2- fold increase
ca15a	No change	No change
ca17a	No change	No change

Table 4.4. Effects of low pH on the regulation of major ion transporters in whole zebrafish larvae and HR cells in present study

Ion transporters	Whole fish (pH 4 vs. pH 7.6)	HR cells (pH 4 vs pH 7.6)
h^+-atpase	5-fold increase	8 -fold increase
nhe3b	No change	4- fold increase
rhcgb	5- fold increase	15 -fold increase
ca15a	5 -fold increase	10 -fold increase
ca17a	5 -fold increase	23- fold increase

Appendix

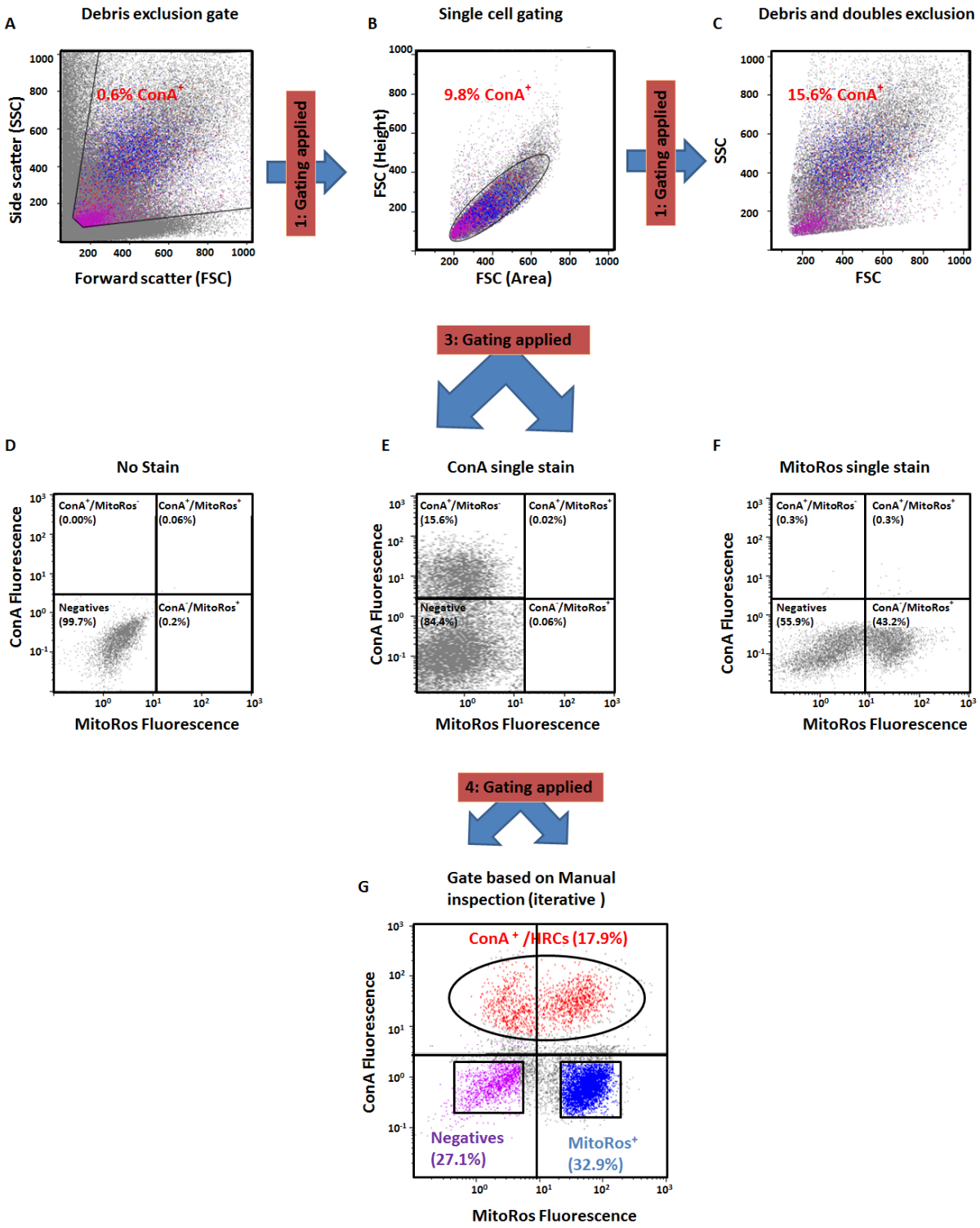
A
Debris exclusion gate
0.6% ConA+
Side scatter (SSC)
Forward scatter (FSC)
1: Gating applied
B
Single cell gating
9.8% ConA+
FSC (Height)
FSC (Area)
1: Gating applied
C
Debris and doubles exclusion
15.6% ConA+
SSC
FSC
3: Gating applied
D
No Stain
ConA+/MitoRos- (0.00%)
ConA+/MitoRos+ (0.06%)
Negatives (99.7%)
ConA-/MitoRos+ (0.2%)
ConA Fluorescence
MitoRos Fluorescence
E
ConA single stain
ConA+/MitoRos- (15.6%)
ConA+/MitoRos+ (0.02%)
Negative (84.4%)
ConA-/MitoRos+ (0.06%)
ConA Fluorescence
MitoRos Fluorescence
F
MitoRos single stain
ConA+/MitoRos- (0.3%)
ConA+/MitoRos+ (0.3%)
Negatives (55.9%)
ConA-/MitoRos+ (43.2%)
ConA Fluorescence
MitoRos Fluorescence
4: Gating applied
G
Gate based on Manual inspection (iterative)
ConA+ /HRCs (17.9%)
Negatives (27.1%)
MitoRos+ (32.9%)
ConA Fluorescence
MitoRos Fluorescence

Figure A1. Flow cytometry gating strategy for cells isolated from 4 dpf zebrafish. (A): A scatter plot showing the total population of dissociated 4 dpf zebrafish cells while region of interest was selected to exclude debris based on size and granularity of distribution of total events (total population of cells without any gates exhibit 0.6% $ConA^{+}$). (B) Region of interest was selected to include single cells based on pulse geometry gating using size and granularity from forward scatter (height) and forward scatter (area; FSC-H x FSC-A; refer to "gating strategy" in materials and methods) (exhibit 9.8% $ConA^{+\ after}$ exclusion of debris). (C) A representative scatter plot with exclusion of cell debris and doublet (exhibit 15.6% $ConA^{+}$ after exclusion of debris and double events). (D) A representative scatter plot obtained from cells isolated from unstained fish to determine the gate setttings (fluorescence boundaries) for delineating negative (unstained) and positve (ConA and/or MitoRos stained) cells using sorting gates pre-determined to be selective for ConA and MitoRos. (E) A representative scatter plot obtained using cells derived from fish singly stained with ConA indicating that the dissociated cell population exhibited 15.6% ConA positive ($ConA^{+}$) cells with only 0.06% being MitoRos positve ($MitoRos^{+}$; non-specific fluorescence). (F) A representative scatter plot obtained using cells derived from fish singly stained with MitoRos indicating that the dissociated cell population exhibited 32.9% $MitoRos^{+}$ cells with only 0.3% being $ConA^{+}$ (non-specific fluorescence). (G) Scatter plot showing sorting gates based on manual inspection derived from B-F, three populations of cells were sorted as indicated by the different colours; $ConA^{+}$ cells (either $MitoRos^{+}$ or $MitoRos^{-}$; HR cells) (red), $MitoRos^{+}/ConA^{-}$ cells (non-HRC ionocytes; blue) and $MitoRos^{-}/ConA^{-}$ cells (non-ionocytes; purple).Note: the threshold being set by manual inspection will vary little between individual run.

A

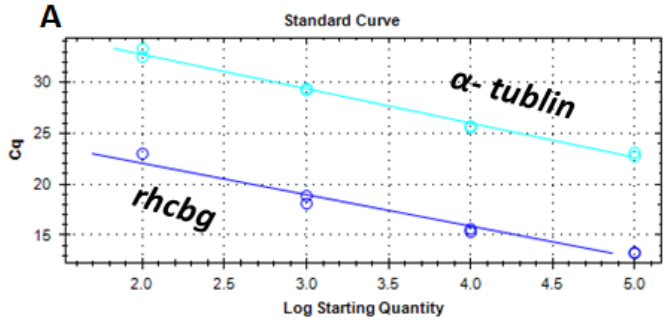

B

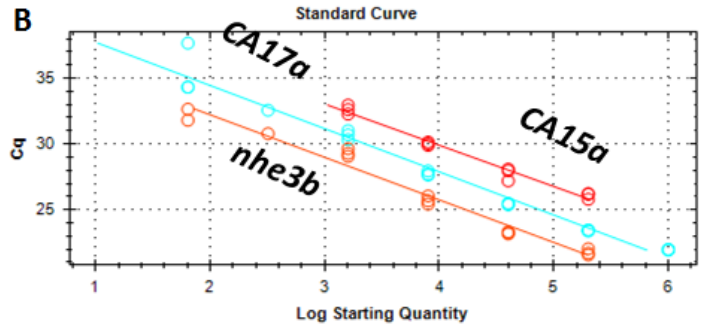

C

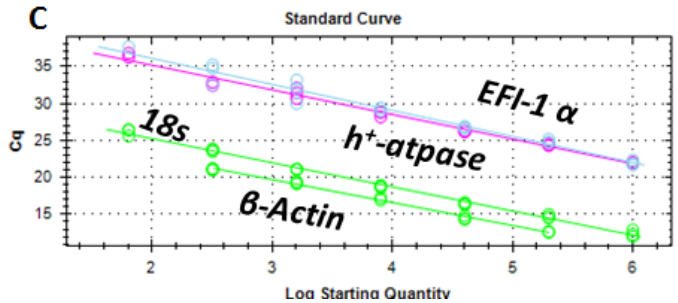

D

GENE	Efficiency %	r2
α-tublin	98.1%	0.992
rhcbg	110.9%	0.966
CA15a	103.7%	0.971
CA17a	101.5%	0.973
nhe3b	108.3%	0.980
18s	109.7%	0.995
β-Actin	102.5%	0.995
EFI-1 α	92.3%	0.972
h^+-atpase	99.6%	0.986

Figure A2. The efficiency of the different primer sets: (A-C): The linear relationship between log concentration and Ct values for a series of dilutions using primer sets for gene of interests. Each dilution for standard was assayed in duplicate by quantitative RT-PCR using 50 ng of total mRNA of HR cells. All r^2 values were >0.970 and all amplification efficiency were ~ 90-110%. D: the summarized efficiency percentage and r^2 value for each primer set.

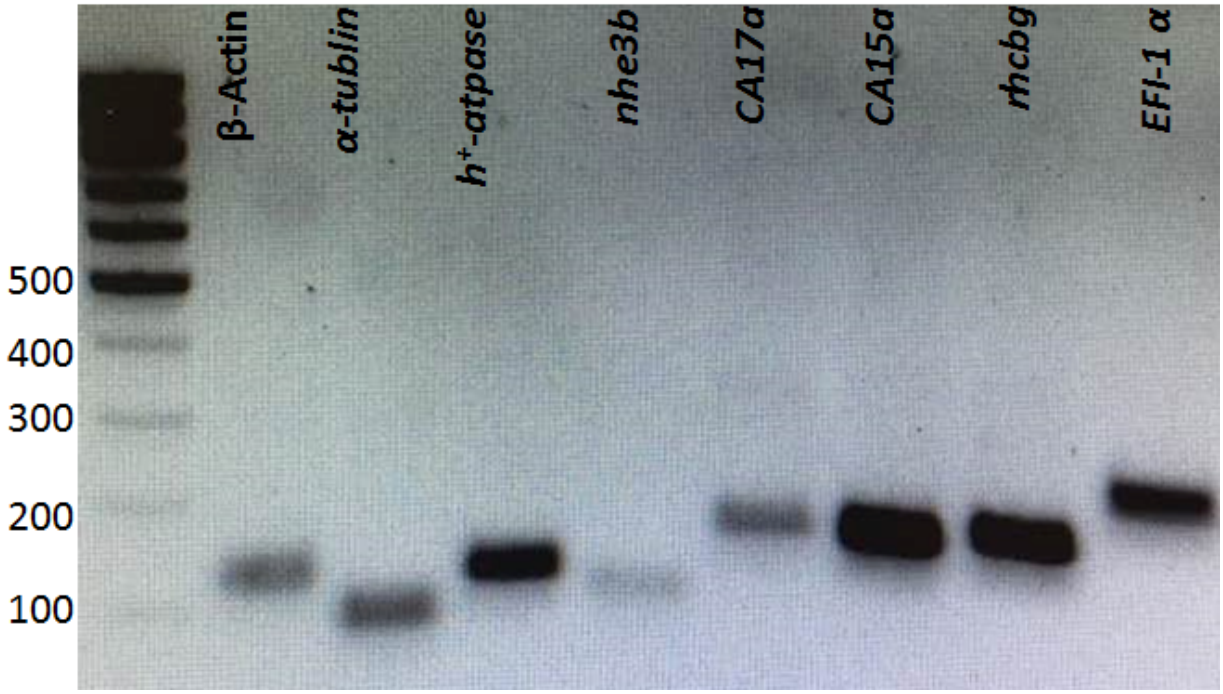
500
400
300
200
100
β-Actin
α-tublin
h+-atpase
nhe3b
CA17a
CA15a
rhcbg
EFI-1 α

Figure A3. Representative agarose gel electrophoresis to check the efficiency of the primers used in RT-qPCR assay. Representative images of qPCR products for 4dpf zebrafish genes carried out on cDNA synthesized from RNA extracted from HR cells. There no nonspecific bands present for each product. The names on top the lanes represent the product of the gene which PCR was carried out. For all genes; the sizes of product were matched with the expected product sizes.

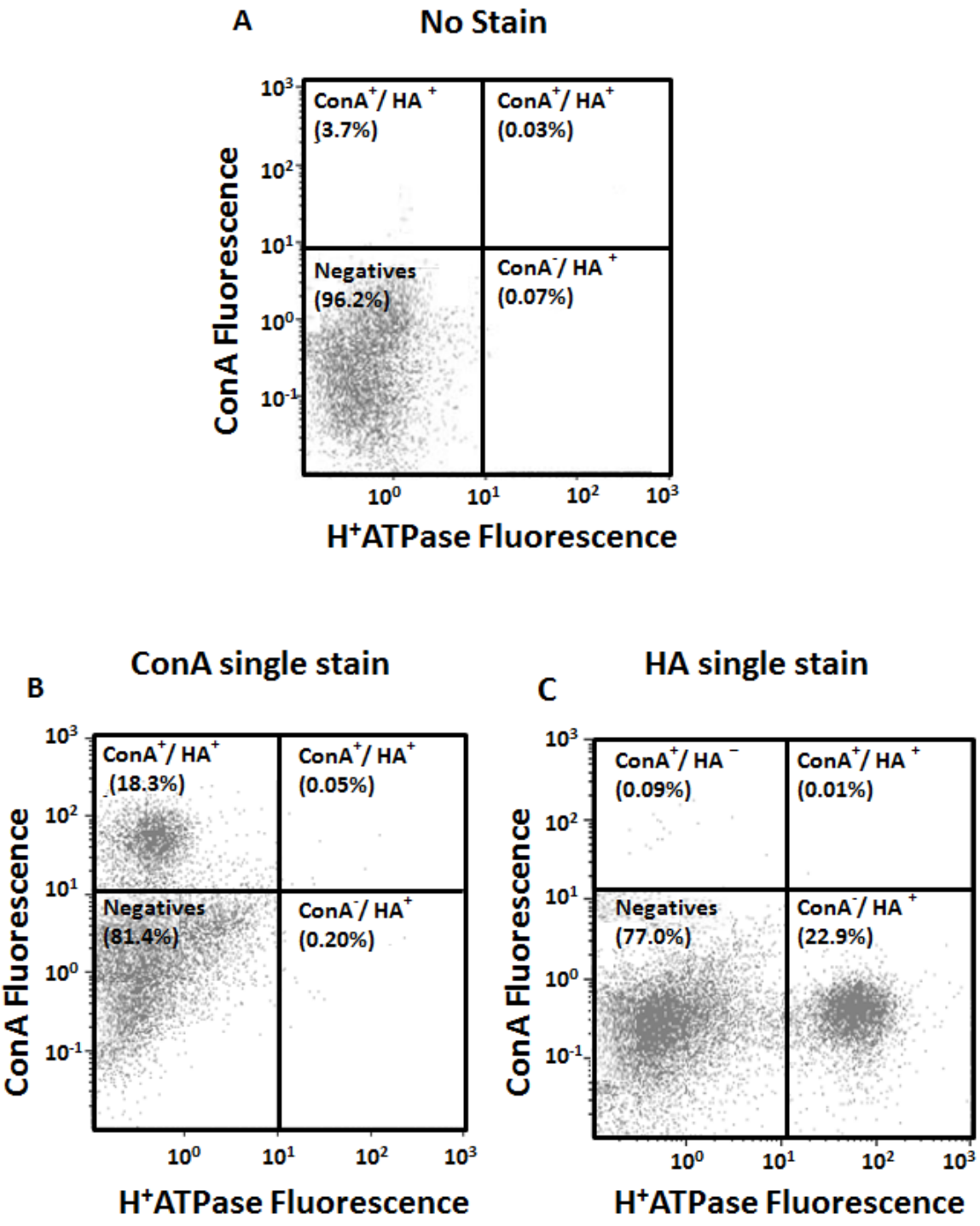
A
No Stain
ConA+/ HA +
(3.7%)
ConA+/ HA+
(0.03%)
Negatives
(96.2%)
ConA-/ HA +
(0.07%)
ConA Fluorescence
H+ATPase Fluorescence
B
ConA single stain
ConA+/ HA+
(18.3%)
ConA+/ HA+
(0.05%)
Negatives
(81.4%)
ConA-/ HA+
(0.20%)
ConA Fluorescence
H+ATPase Fluorescence
C
HA single stain
ConA+/ HA −
(0.09%)
ConA+/ HA +
(0.01%)
Negatives
(77.0%)
ConA-/ HA +
(22.9%)
ConA Fluorescence
H+ATPase Fluorescence

Figure A4. **Representative flow cytometery data of unstained and singly stained (H^+-ATPase or ConA) cells isolated from from zebrafish larvae at 4 dpf.** (A) Scatterplot of cell distributions obtained from unstained cells isolated from zebrafish larvae at 4 dpf using sorting gates pre-determined to be selective for H^+-ATPase and ConA. (B) Representative scatterplot obtained for the ConA stained sample indicating that the dissociated cell population exhibited 18.3% $ConA^+$ cells with only 0.2% being H^+-$ATPase^+$ (non-specific fluorescence). (C) Representative scatterplot obtained from dissociated cells that were stained forH^+-ATPase indicating that the dissociated cell population exhibited 22.9% H^+-$ATPase^+$ cells with only 0.1% being $ConA^+$ (non-specific fluorescence).

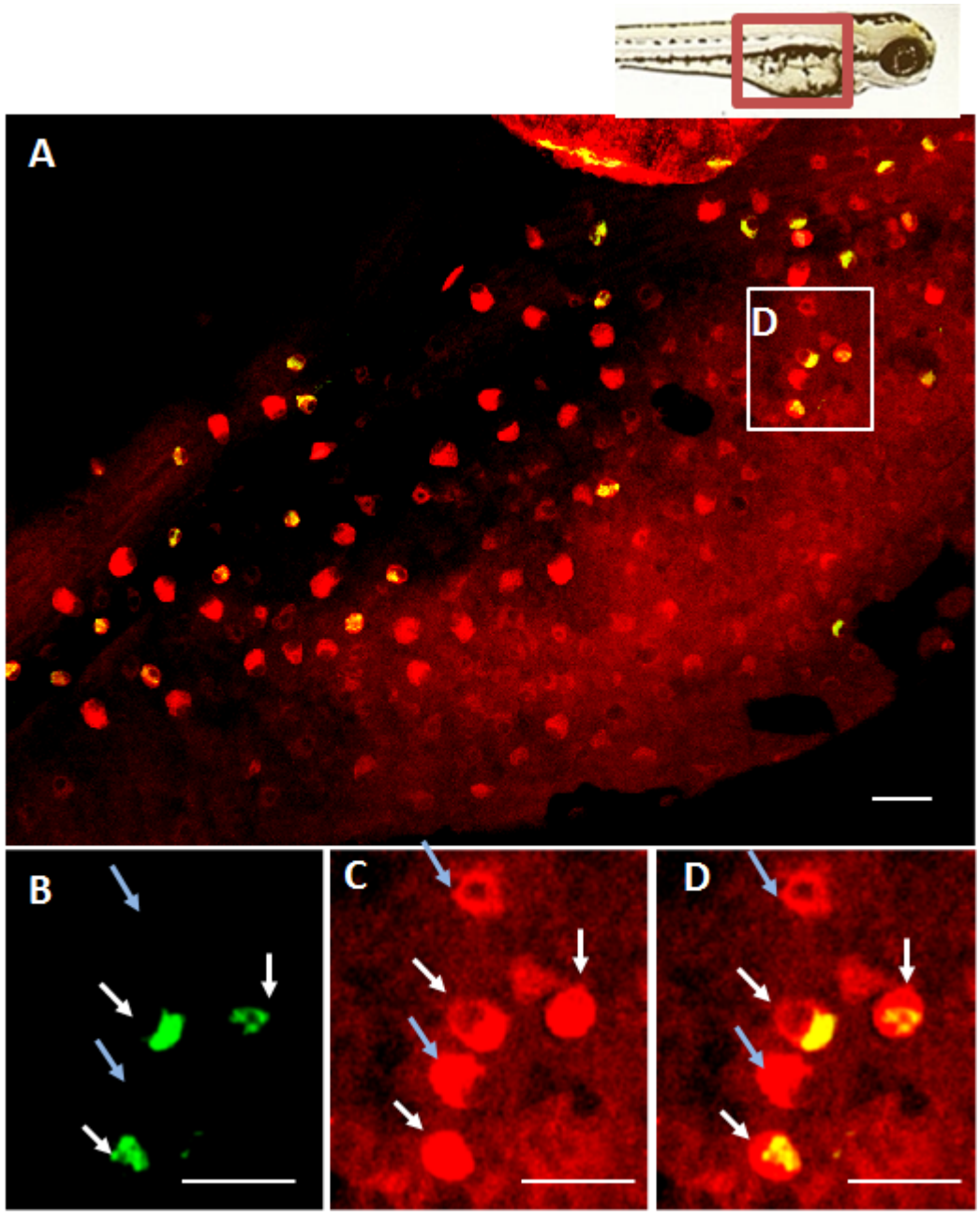
A
D
B
C
D

Figure A5: Confocal images of Na^+/Cl^- co-transporting (NCC) antibody (Stains Na^+/Cl^- co-transporting cells (NCCC) and MitoRos (Stains the Mitochondria of ionocytes) on the skin of a wild type 4 dpf zebrafish larvae (*Danio rerio*). (A): double immunofluorescence staining for MitoRos and NCC antibody indicates staining of MitoRos and NCC antibody in yolk sac of 4 dpf larval zebrafish *(Danio rerio*). (B):Zoomed image of NCC staining in yolk sac of 4 dpf larval zebrafish. (C): Zoomed image of MitoRos in yolk sac of 4dpf larval zebrafish (D): Zoomed images of Colocalization of NCC and MitoRos, the white arrows indicate cells positive for both NCC and MitoRos, blue arrows indicate cells positive for both only MitoRos. Scale bar 20 µm.

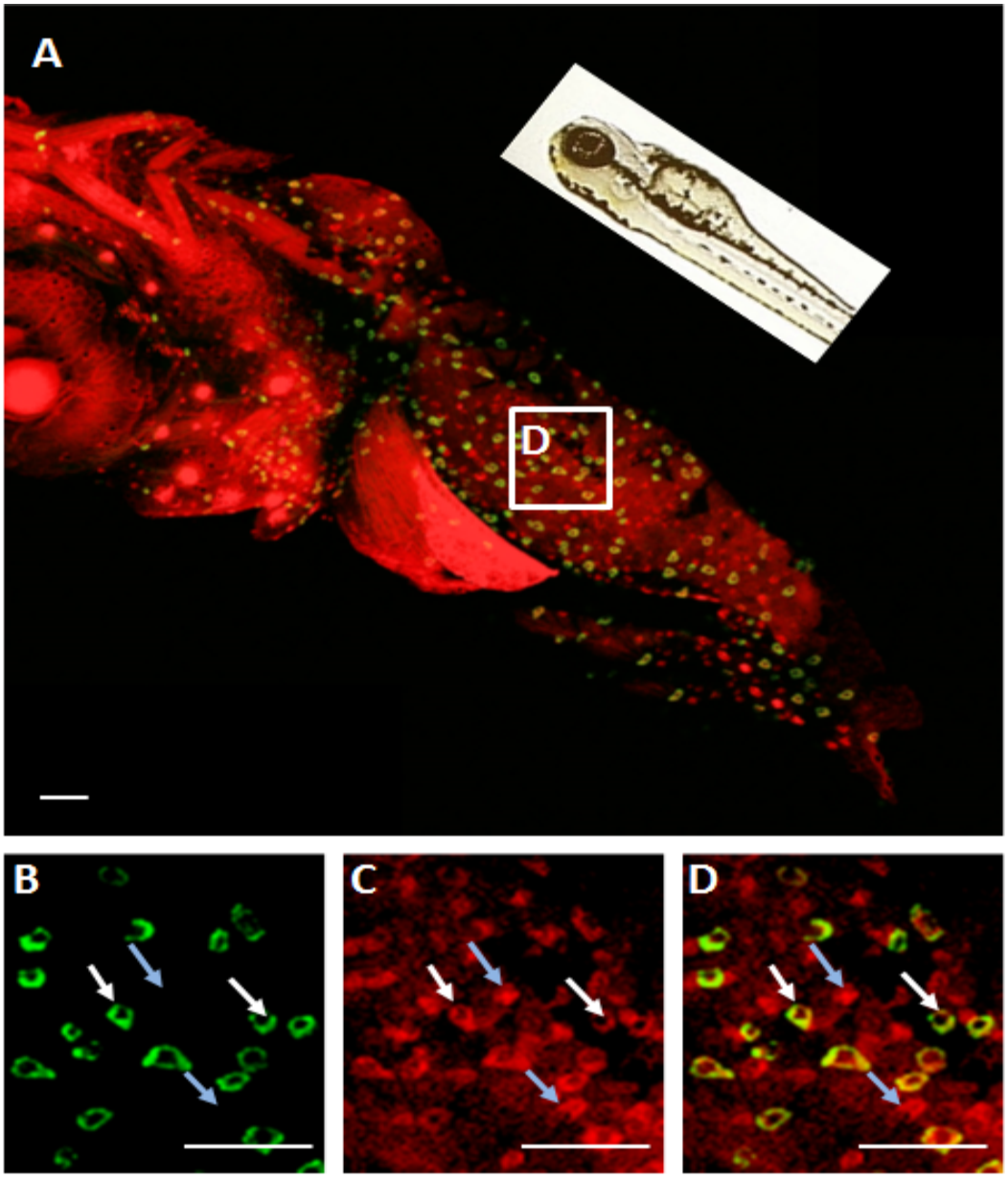
A
D
B
C
D

Figure A6: Confocal images of Na^+/K^+-ATPase (NaR) antibody (stains the Na^+/K^+-ATPase rich cells) and MitoRos(Stains the Mirochondira of ionocytes in zebrafish) on the skin of a wild type 4 dpf zebrafish larvae (*Danio rerio*). (A): double immunofluorescence staining for MItoRos and NaR antibody indicates staining of MitoRos and NaR antibody in whole 4 dpf larval zebrafish *(Danio rerio*). (B): Close up image of the NaR antibody staining in yolk sac of 4 dpf larval zebrafish. (C): close up image of MitoRos staining in yolk sac of 4dpf larval zebrafish (E): close up image of Colocalization of NaR, MitoRos stains in yolk sac of 4dpf larval zebrafish, the white arrows indicate cells positive for both NaR and MitoRos, blue arrows indicate cells positive for both only MitoRos. Scale bar 20 µm.

Bibliography

Abbas, L., Hajihashemi, S., Stead, L. F., Cooper, G. J., Ware, T. L., Munsey, T. S., Whitfield, T. T. and White, S. J. (2011). Functional and developmental expression of a zebrafish Kir1.1 (ROMK) potassium channel homologue Kcnj1. *Journal of Physiology* **589**, 1489–1503.

Bayaa, M., Vulesevic, B., Esbaugh, A., Braun, M., Ekker, M. E., Grosell, M. and Perry, S. F. (2009). The involvement of SLC26 anion transporters in chloride uptake in zebrafish (Danio rerio) larvae. *Journal of Experimental Biology* **212**, 3283–3295.

Bill, B. R., Petzold, A. M., Clark, K. J., Schimmenti, L. A. and Ekker, S. C. (2009). A Primer for Morpholino Use in Zebrafish. *Zebrafish* **6**, 69–77.

Boisen, A. M. Z., Amstrup, J., Novak, I. and Grosell, M. (2003). Sodium and chloride transport in soft water and hard water acclimated zebrafish (Danio rerio). In *Biochimica et Biophysica Acta - Biomembranes*.**1618(2)**:207-18.

Carrie, D. and Gilmour, K. M. (2016). Phosphorylation increases the catalytic activity of rainbow trout gill cytosolic carbonic anhydrase. *Journal of Comparative Physiology B: Biochemical, Systemic, and Environmental Physiology*.**186(1)**:111-22.

Chang, W.-J., Horng, J.-L., Yan, J.-J., Hsiao, C.-D. and Hwang, P.-P. (2009). The transcription factor, glial cell missing 2, is involved in differentiation and functional regulation of H+-ATPase-rich cells in zebrafish (Danio rerio). *AJP: Regulatory, Integrative and Comparative Physiology* **296**, R1192–R1201.

Chang, W. J., Wang, Y. F., Hu, H. J., Wang, J. H., Lee, T. H. and Hwang, P. P. (2013). Compensatory regulation of Na+ absorption by Na+/H+ exchanger and Na+-Cl- cotransporter in zebrafish

(Danio rerio). *Frontiers in Zoology*.**10**:46

Chasiotis, H., Kolosov, D. and Kelly, S. P. (2012). Permeability properties of the teleost gill epithelium under ion-poor conditions. *American Journal of Physiology-Regulatory, Integrative and Comparative Physiology* **302**, R727–R739.

Chou, M.-Y., Hsiao, C.-D., Chen, S.-C., Chen, I.-W., Liu, S.-T. and Hwang, P.-P. (2008). Effects of hypothermia on gene expression in zebrafish gills: upregulation in differentiation and function of ionocytes as compensatory responses. *Journal of Experimental Biology* **211**, 3077–3084.

Craig, P. M., Wood, C. M. and McClelland, G. B. (2007). Gill membrane remodeling with soft-water acclimation in zebrafish (Danio rerio). *Physiological genomics* **30**, 53–60.

Cruz, S. A., Chao, P. L. and Hwang, P. P. (2013). Cortisol promotes differentiation of epidermal ionocytes through Foxi3 transcription factors in zebrafish (Danio rerio). *Comparative Biochemistry and Physiology - A Molecular and Integrative Physiology* **164**, 249–257.

David, L. E., Fowler, C. B., Cunningham, B. R., Mason, J. T. and O'Leary, T. J. (2011). The effect of formaldehyde fixation on RNA: Optimization of formaldehyde adduct removal. *Journal of Molecular Diagnostics*.3(3): 282–288

Dymowska, A. K., Hwang, P. P. and Goss, G. G. (2012). Structure and function of ionocytes in the freshwater fish gill. *Respiratory Physiology and Neurobiology* **184**, 282–292.

Eisen, J. S. and Smith, J. C. (2008). Controlling morpholino experiments: don't stop making antisense. *Development* **135**, 1735–1743.

Ekker, M. and Akimenko, E. (2010). Genetic tools. *Zebrafish: FISH PHYSIOLOGY* **29**, 1–23.

Esaki, M., Hoshijima, K., Nakamura, N., Munakata, K., Tanaka, M., Ookata, K., Asakawa, K., Kawakami, K., Wang, W., Weinberg, E. S., et al. (2009). Mechanism of development of ionocytes rich in vacuolar-type H+-ATPase in the skin of zebrafish larvae. *Developmental Biology* **329**, 116–129.

A. J. Esbaugh, S. F. Perry, M. Bayaa, T. Georgalis, J. Nickerson, B. L. Tufts, K. M. Gilmour. (2005). Cytoplasmic carbonic anhydrase isozymes in rainbow trout Oncorhynchus mykiss: comparative physiology and molecular evolution. *Journal of Experimental Biology*. **208**, 1951-1961

Fredriksson, S., Gullberg, M., Jarvius, J., Olsson, C., Pietras, K., Gústafsdóttir, S. M., Östman, A. and Landegren, U. (2002). Protein detection using proximity-dependent DNA ligation assays. *Nature Biotechnology*. **20(5)**, 473-7.

Gilmour, K. M., Collier, C. L., Dey, C. J. and Perry, S. F. (2011). Roles of cortisol and carbonic anhydrase in acid-base compensation in rainbow trout, Oncorhynchus mykiss. *Journal of Comparative Physiology B: Biochemical, Systemic, and Environmental Physiology* **181**, 501–515.

Guh, Y.-J., Lin, C.-H. and Hwang, P.-P. (2015). Osmoregulation in zebrafish: ion transport mechanisms and functional regulation. *EXCLI journal* **14**,627–659.

Horng, J. L. and Lin, L. Y. (2008). Expression of the Na-K-2Cl Cotransporter in Branchial Mitochondrion-Rich Cells of Mozambique Tilapia (_Oreochromis mossambicus_) Subjected to Varying Chloride Conditions. *Zoological Studies* **47**, 733–740.

Horng, J.-L., Lin, L.-Y., Huang, C.-J., Katoh, F., Kaneko, T. and Hwang, P.-P. (2007). Knockdown of V-ATPase subunit A (atp6v1a) impairs acid secretion and ion balance in zebrafish (Danio

rerio). *American Journal of Physiology. Regulatory, Integrative and Comparative Physiology* **292**, R2068-2076.

Horng, J.-L., Lin, L.-Y. and Hwang, P.-P. (2009). Functional regulation of H+-ATPase-rich cells in zebrafish embryos acclimated to an acidic environment. *American journal of physiology. Cell physiology* **296**, C682–C692.

Hoshijima, K. and Hirose, S. (2007). Expression of endocrine genes in zebrafish larvae in response to environmental salinity. *Journal of Endocrinology* **193**, 481–491.

Hsu, H. H., Lin, L. Y., Tseng, Y. C., Horng, J. L. and Hwang, P. P. (2014). A new model for fish ion regulation: Identification of ionocytes in freshwater- and seawater-acclimated medaka (Oryzias latipes). *Cell and Tissue Research* **357**, 225–243.

Hwang, P. P. (2009). Ion uptake and acid secretion in zebrafish (Danio rerio). *Journal of Experimental Biology* **212**, 1745–1752.

Hwang, P.-P. and Chou, M.-Y. (2013). Zebrafish as an animal model to study ion homeostasis. *Pflügers Archiv - European Journal of Physiology* **465**, 1233–1247.

Hwang, P.-P. and Perry, S. F. (2010). *8 – Ionic and acid–base regulation*.

Hwang, P.-P., Lee, T.-H., Lin, L.-Y., Alper, S., Anderson, J., Itallie, C. van, Avella, M., Bornancin, M., Bagherie-Lachidan, M., Wright, S., et al. (2011). Ion regulation in fish gills: recent progress in the cellular and molecular mechanisms. *American journal of physiology. Regulatory, integrative and comparative physiology* **301**, R28-47.

Ito, Y., Kobayashi, S., Nakamura, N., Miyagi, H., Esaki, M., Hoshijima, K. and Hirose, S. (2013). Close association of carbonic anhydrase (CA2a and ca15a), Na+/h+exchanger (Nhe3b), and ammonia transporter Rhcg1 in zebrafish ionocytes responsible for na+uptake. *Frontiers in*

Physiology **4 ,** 39.

Kumai, Y. and Perry, S. F. (2011). Ammonia excretion via Rhcg1 facilitates Na+ uptake in larval zebrafish, Danio rerio, in acidic water. *AJP: Regulatory, Integrative and Comparative Physiology* **301**, R1517–R1528.

Kumai, Y. and Perry, S. F. (2012a). Mechanisms and regulation of Na+ uptake by freshwater fish. *Respiratory Physiology & Neurobiology* **184**, 249–256.

Kumai, Y. and Perry, S. F. (2012b). Mechanisms and regulation of Na+uptake by freshwater fish. *Respiratory Physiology and Neurobiology* **184**, 249–256.

Kumai, Y., Bahubeshi, A., Steele, S. and Perry, S. F. (2011). Strategies for maintaining Na+ balance in zebrafish (Danio rerio) during prolonged exposure to acidic water. *Comparative Biochemistry and Physiology - A Molecular and Integrative Physiology* **160**, 52–62.

Kumai, Y., Ward, M. A. R. and Perry, S. F. (2012). -Adrenergic regulation of Na+ uptake by larval zebrafish Danio rerio in acidic and ion-poor environments. *AJP: Regulatory, Integrative and Comparative Physiology* **303**, R1031–R1041.

Kwong, R. W. M. and Perry, S. F. (2016). A role for sodium-chloride cotransporters in the rapid regulation of ion uptake following acute environmental acidosis: new insights from the zebrafish model. *American Journal of Physiology - Cell Physiology*. 311(6), 931-941

Kwong, R. W. M., Kumai, Y. and Perry, S. F. (2014). The physiology of fish at low pH: the zebrafish as a model system. *Journal of Experimental Biology* **217**, 651–662.

Laurent, P. and Perry, S. F. (1991). Environmental effects on fish gill morphology. *Physiological Zoology*. **64(1)**, 4-25

Liao, B. K., Deng, A. N., Chen, S. C., Chou, M. Y. and Hwang, P. P. (2007). Expression and water

calcium dependence of calcium transporter isoforms in zebrafish gill mitochondrion-rich cells. *BMC Genomics* **8**,.354-360

Lin, L.-Y. (2005). Proton pump-rich cell secretes acid in skin of zebrafish larvae. *AJP: Cell Physiology*. **290(2)**, 371-378

Lin, T.-Y., Liao, B.-K., Horng, J.-L., Yan, J.-J., Hsiao, C.-D. and Hwang, P.-P. (2008). Carbonic anhydrase 2-like a and 15a are involved in acid-base regulation and Na^+ uptake in zebrafish H^+-ATPase-rich cells. *American Journal of Physiology-Cell Physiology* **294**, C1250–C1260.

Lin, C. H., Shih, T. H., Liu, S. T., Hsu, H. H. and Hwang, P. P. (2015). Cortisol regulates acid secretion of H+-ATPase-rich ionocytes in Zebrafish (Danio rerio) embryos. *Frontiers in Physiology* **6**, 326-334

McCurley , Amy T and Callard, Gloria v (2008). Characterization of housekeeping genes in zebrafish: male-female differences and effects of tissue type, developmental stage and chemical treatment *BMC Molecular Biology* **9**:102-110

McDonald, D. G. and Rogano, M. S. (1986). Ion Regulation by the Rainbow Trout, Salmo gairdneri, in Ion-Poor Water. *Physiological Zoology*. **58 (3)**, 318-331

Nakada, T., Hoshijima, K., Esaki, M., Nagayoshi, S., Kawakami, K. and Hirose, S. (2007). Localization of ammonia transporter Rhcg1 in mitochondrion-rich cells of yolk sac, gill, and kidney of zebrafish and its ionic strength-dependent expression. *AJP: Regulatory, Integrative and Comparative Physiology* **293**, R1743–R1753.

Nawata, C. M., Hung, C. C. Y., Tsui, T. K. N., Wilson, J. M., Wright, P. A. and Wood, C. M. (2007). Ammonia excretion in rainbow trout (Oncorhynchus mykiss): evidence for Rh glycoprotein and H+-ATPase involvement. *Physiological Genomics* **31**, 463–474.

Pan, T.-C., Liao, B.-K., Huang, C.-J., Lin, L.-Y. and Hwang, P.-P. (2005). Epithelial Ca(2+) channel expression and Ca(2+) uptake in developing zebrafish. *American journal of physiology. Regulatory, integrative and comparative physiology* **289**, R1202–R1211.

Perry, S. and Laurent, P. (1989). Adaptational responses of rainbow trout to lowered external NaCl concentration: contribution of the branchial chloride cell. *Journal of Experimental Biology* **147**, 147–168.

Perry, S. F., Vulesevic, B., Grosell, M. and Bayaa, M. (2009). Evidence that SLC26 anion transporters mediate branchial chloride uptake in adult zebrafish (Danio rerio). *AJP: Regulatory, Integrative and Comparative Physiology* **297**, R988–R997.

Shih, T.-H., Horng, J.-L., Hwang, P.-P. and Lin, L.-Y. (2008). Ammonia excretion by the skin of zebrafish (Danio rerio) larvae. *American journal of physiology. Cell physiology* **295**, C1625-32.

Shih, T.-H., Horng, J.-L., Liu, S.-T., Hwang, P.-P. and Lin, L.-Y. (2012a). Rhcg1 and NHE3b are involved in ammonium-dependent sodium uptake by zebrafish larvae acclimated to low-sodium water. *AJP: Regulatory, Integrative and Comparative Physiology* **302**, R84–R93.

Shih, T.-H., Horng, J.-L., Liu, S.-T., Hwang, P.-P., Lin, L.-Y., Avella, M., Bornancin, M., Esaki, M., Hoshijima, K., Kobayashi, S., et al. (2012b). Rhcg1 and NHE3b are involved in ammonium-dependent sodium uptake by zebrafish larvae acclimated to low-sodium water. *American journal of physiology. Regulatory, integrative and comparative physiology* **302**, R84-93.

Suster, M. L., Kikuta, H., Urasaki, A., Asakawa, K. and Kawakami, K. (2009). Transgenesis in Zebrafish with the Tol2 transposon system. *Methods in Molecular Biology* **561**, 41–63.

Wang, Y. F., Tseng, Y. C., Yan, J. J., Hiroi, J. and Hwang, P. P. (2009). Role of SLC12A10.2, a Na-Cl

cotransporter-like protein, in a Cl uptake mechanism in zebrafish (_Danio rerio_). *American Journal of Physiology - Regulatory Integrative & Comparative Physiology* **296**, R1650–R1660.

Weiner, I. D., Verlander, J. W., Arena, E. A., Longo, W. E., Roberts, K. E., Geibel, P., Nateqi, J., Geibel, J. P., Han, K., Lee, H., et al. (2012). Role of NH 3 and NH 4 + transporters in renal acid-base transport. *Renal Physiology*. **300 (1)**, 11-23

Wright, P. A. and Wood, C. M. (2009). A new paradigm for ammonia excretion in aquatic animals: role of Rhesus (Rh) glycoproteins. *Journal of Experimental Biology.* **212**, 2303-12

Wright, P. A., Randall, D. J. and Perry, S. F. (1989). Fish gill water boundary layer: a site of linkage between carbon dioxide and ammonia excretion. *Journal of Comparative Physiology B*. **158(6)**, 627-635

Wu, S., Horng, J., Liu, S., Hwang, P., Wen, Z., Lin, C. and Lin, L. (2010). Ammonium-dependent sodium uptake in mitochondrion-rich cells of medaka (Oryzias latipes) larvae. *American Phyiological Society*. **298(2)**, C237-C250

Yan, J.-J., Chou, M.-Y., Kaneko, T. and Hwang, P.-P. (2007). Gene expression of Na+/H+ exchanger in zebrafish H+ -ATPase-rich cells during acclimation to low-Na+ and acidic environments. *American journal of physiology. Cell physiology* **293**, C1814-23.

Zimmer, A. M., Dymowska, A. K., Kumai, Y., Goss, G. G., Perry, S. F. and Kwong, R. W. M. (2018). Assessing the role of the acid-sensing ion channel ASIC4b in sodium uptake by larval zebrafish. *Comparative Biochemistry and Physiology -Part A : Molecular and Integrative Physiology*.**226**,1-10